A ONE-DIMENSIONAL MODEL FOR ODD NITROGEN IN THE STRATOSPHERE, MESOSPHERE, AND THERMOSPHERE

by

CASIMIR RICHARD BULIKOWSKI

B.S., University of Massachusetts at Amherst
(1971)

M.S., Northwestern University
(1973)

SUBMITTED IN PARTIAL FULFILLMENT
OF THE REQUIREMENTS FOR THE
DEGREE OF

MASTER OF SCIENCE

at the

MASSACHUSETTS INSTITUTE OF TECHNOLOGY

(August, 1977)

Signature of Author.....
Department of Meteorology, August 29, 1977

Certified by.....
Thesis Supervisor

Accepted by.....
Chairman, Department Committee

A ONE-DIMENSIONAL MODEL FOR ODD NITROGEN IN THE STRATOSPHERE, MESOSPHERE, AND THERMOSPHERE

by

CASIMIR RICHARD BULIKOWSKI

Submitted to the Department of Meteorology
on August 29, 1977 in partial fulfillment of the requirements
for the Degree of Master of Science

ABSTRACT

A new method is demonstrated for solving a one-dimensional chemical-dynamical model for odd nitrogen in the upper stratosphere, mesosphere, and lower thermosphere. Essentially, the method involves time integrating a photochemical-diffusive equation through dissimilar daytime and nighttime regimes by means of the Lorenz N-cycle scheme. The model uses average daytime and nighttime input data instead of time-dependent data or diurnally averaged data. The system results in a steady-state solution in the upper stratosphere and lower mesosphere and a pseudo steady-state solution in the upper mesosphere and lower thermosphere. The results should be more physically realistic than those obtained from a model which utilizes diurnally averaged data. Some of the chemical and dynamical processes are also investigated by changing the eddy diffusion coefficient and changing the fraction of $N(^4S)$ produced from the dissociative recombination of NO^+.

Thesis Supervisor: Ronald G. Prinn
Title: Associate Professor of Meteorology

TABLE OF CONTENTS

LIST OF FIGURES

LIST OF TABLES

1. Introduction

One of the significant problems aeronomers have faced in stratospheric-mesospheric modelling is how to treat diurnal variations in sunlight intensity in order to predict the most realistic species concentrations. A number of approaches have been used including calculating the photolysis rates using the approximation of a mean solar zenith angle, obtaining the photodissociation rates by numerically integrating them over a diurnal cycle, and obtaining a diurnally time-dependent solution. Of the three, the last approach is the most realistic; but it is also the most expensive and is not without problems, such as handling the sunrise and sunset transitions. The first two approaches do not treat nighttime processes adequately, if at all, and presumably give concentrations which are averaged over a 24-hour day, thus making it difficult to compare these values with daytime values. Furthermore, the average predicted concentration values often differ by as much as 50 percent from the average values computed from a time-dependent solution because of the inherent difficulties in averaging photodissociation rates over a diurnal cycle.

Here we will demonstrate a new method for solving a one-dimensional chemical-dynamical model for odd nitrogen in the upper stratosphere, mesosphere, and lower thermosphere. The resultant model is a diurnally time-dependent one which simulates nighttime processes but uses average daytime and nighttime input data, observational wherever possible. Essentially, the method involves the time integration of a photochemical-diffusive equation by means of the N-cycle scheme of Lorenz (1971) with

the values computed at the end of the daytime used as the initial values for the nighttime integration and vice versa. The system results in a steady-state solution in the upper stratosphere and lower mesosphere and a pseudo steady-state solution in the upper mesosphere and lower thermosphere. In other words, the concentration remains constant throughout the daytime and nighttime in the steady-state regime and varies cyclically in the pseudo steady-state regime. The average values thus obtained should be more physically realistic than values obtained from a solution which averages photolysis rates over a 24-hour day either by integration or by use of a mean solar zenith angle.

In addition to the viability of this method being demonstrated, some of the physical processes in the odd nitrogen system are also investigated since odd nitrogen plays an important role in the catalytic destruction of ozone.

2. Input Data

The reactions which are used in the odd nitrogen model are presented in Table 1. Almost twice as many reactions were initially considered for the model, but the other reactions were not included because they were shown to be negligible in their effects when compared to the included reactions. Even some of the included reactions have little impact on the results, as we shall see later. An attempt was made to obtain the best available rate constants and photolysis rates. Many of the rate constants were taken from data surveys prepared for the Climatic Impact Assessment Program, Department of Transportation.

Some of the reaction rates were not included in the table and can be found in Appendix A. Photolysis rate J_1 was calculated by Strobel (1971b) at a 60° solar zenith angle. This angle was chosen to represent a mid-latitude, daytime average sunlight intensity. Photolysis rate J_7 was evaluated by Cieslik and Nicolet (1973) at a 60° zenith angle in detailed calculations based on the absorption of the discrete Schumann-Runge bands of O_2. Diurnal mean values for rates J_{13} and J_{58} were calculated by Prinn et al. (1975) in a modified version of their model extended to 68 km. The rates were multiplied by 2 to obtain daytime values. Rate J_{13} did not vary significantly over the height range of interest so that a constant value was used. The production rate of nitrogen atoms by electron impact dissociation of N_2, r_{31}, was obtained from a table and graph by Strobel et al. (1970) and Strobel (1971b), respectively. Their values were divided by 2 in order to represent the production rate of one $N(^4S)$ atom or one $N(^2D)$ atom, following the discussion by Oran et al. (1975). The rate constant for the dissociative

Table 1. Reactions, photodissociation rates, rate constants and references. Photodissociation rates have units sec^{-1}. Rate constants have units cm^6 sec^{-1} and cm^3 sec^{-1} for 3- and 2-body reactions, respectively.

Reaction	Rate	Reference
1. $N_2 + h\nu(1098\text{-}1249\text{Å}) \rightarrow N(^4S) + N(^4S)$	J_1 (see text)	Strobel (1971b)
2. $N(^4S) + NO \rightarrow N_2 + O$	$k_2=1.5\times10^{-12}T^{\frac{1}{2}}$	Phillips and Schiff (1962)
3. $N(^4S) + O_2 \rightarrow NO + O$	$k_3=1.1\times10^{-14}T\exp(-3150/T)$	Baulch et al. (1973)
4. $N(^4S) + O_2(^1\Delta_g) \rightarrow NO + O$	$k_4=2\times10^{-14}\exp(-6.0\times10^2/T)$	Clark and Wayne (1970)
5. $N(^4S) + O_3 \rightarrow NO + O_2$	$k_5=5.7\times10^{-13}$	Baulch et al. (1973)
7. $NO + h\nu(1750\text{-}1908\text{Å}) \rightarrow N(^4S) + O$	J_7 (see text)	Cieslik and Nicolet (1973)
9. $N(^2D) + O_2 \rightarrow NO + O$	$k_9=4.4\times10^{-13}T^{\frac{1}{2}}$	Slanger et al. (1971)
10. $NO + O_3 \rightarrow NO_2 + O_2$	$k_{10}=9\times10^{-13}\exp(-1200/T)$	Herron and Huie (1972)
11. $NO + O + M \rightarrow NO_2 + M$	$k_{11}=3.0\times10^{-33}\exp(940/T)$ *	Baulch et al. (1973)
12. $NO + O \rightarrow NO_2 + h\nu$	$k_{12}=4.2\times10^{-18}$	Becker et al. (1973)
13. $NO_2 + h\nu(2396\text{-}3950\text{Å}) \rightarrow NO + O$	$J_{13}=9\times10^{-3}$	Prinn et al. (1975)
14. $N(^4S) + NO_2 \rightarrow$ products	$k_{14}=1.85\times10^{-11}$	Phillips and Schiff (1965)
14a. $N(^4S) + NO_2 \rightarrow N_2O + O$	$k_{14a}=8.0\times10^{-12}$	Phillips and Schiff (1965)
14b. $N(^4S) + NO_2 \rightarrow N_2 + O + O$	$k_{14b}=2.4\times10^{-12}$	Phillips and Schiff (1965)
14c. $N(^4S) + NO_2 \rightarrow N_2 + O_2$	$k_{14c}=1.9\times10^{-12}$	Phillips and Schiff (1965)

Table 1. (Continued)

Reaction	Rate	Reference
14d. $N(^4S) + NO_2 \rightarrow NO + NO$	$k_{14d}=6.1\times10^{-12}$	Phillips and Schiff (1965)
15. $NO_2 + O \rightarrow NO + O_2$	$k_{15}=9.1\times10^{-12}$	Davis et al. (1973)
16. $N(^4S) + OH \rightarrow NO + H$	$k_{16}=5.3\times10^{-11}$	Baulch et al. (1973)
17. $N(^2D) + N_2 \rightarrow N(^4S) + N_2$	$k_{17}=2.3\times10^{-14}$	Husain et al. (1972)
20. $N(^2D) + O \rightarrow N(^4S) + O$	$k_{20}=1.8\times10^{-12}$	Davenport et al. (1976)
25. $N(^4S) + O \rightarrow NO + h\nu$	$k_{25}=2\times10^{-17}$	Banks and Kockarts (1973)
31. $N_2 + e^-(fast) \rightarrow N(^4S) + N(^2D) + e^-$	r_{31} (see text) $^+$	Strobel et al. (1970), Strobel (1971b)
32. $NO^+ + e^- \rightarrow N(^2D) + O$	$k_{32}=3.5\times10^{-7}(T/380)^{-0.5}(A)$	Huang et al. (1975), see text
$\rightarrow N(^4S) + O$	$k_{32}=3.5\times10^{-7}(T/380)^{-0.5}(1-A)$	
34. $N_2^+ + O \rightarrow NO^+ + N(^2D)$	$k_{34}=3.1\times10^{-9}T^{-0.44}$	McFarland et al. (1974)
35. $N_2 + O^+ \rightarrow NO^+ + N(^4S)$	$k_{35}=1.2\times10^{-12}(300/T)$	McFarland et al. (1973)
39. $N(^4S) + O_2^+ \rightarrow NO^+ + O$	$k_{39}=1.8\times10^{-10}$	Goldan et al. (1966)
54. $N_2O + O(^1D) \rightarrow NO + NO$	$k_{54}=1.1\times10^{-10}$	Garvin and Hampson (1974)
55. $NO_2 + OH + M \rightarrow HNO_3 + M$	$k_{55}=\frac{8.5\times10^{-13}\exp(360/T)}{1.5\times10^{18}+[M]}$	Prinn et al. (1975)
56. $HNO_3 + O \rightarrow OH + NO_3$	$k_{56}=1.0\times10^{-11}\exp(-1860/T)$	McConnell and McElroy (1973)

Table 1. (Continued)

Reaction	Rate	Reference
57. $HNO_3 + OH \rightarrow H_2O + NO_3$	$k_{57}=1.3\times10^{-13}$	Garvin and Hampson (1974)
58. $HNO_3 + h\nu(1860\text{-}3450\text{Å}) \rightarrow OH + NO_2$	J_{58} (see text)	Prinn et al. (1975)
59. N_2 + cosmic rays $\rightarrow N(^4S) + N(^4S)$	r_{59} (see text) +	Nicolet (1975)

* Must be multiplied by M efficiency of 1.31.

+ Has units $cm^{-3}\ sec^{-1}$.

recombination of NO^+, k_{32}, is written with an adjustable parameter, A, which is the fraction of the total recombination events resulting in the production of $N(^2D)$ atoms. If A = 1, each event produces one $N(^2D)$ atom and no $N(^4S)$ atoms. If A = 0, the converse occurs. The impact of changes in this parameter is investigated. Finally, r_{59}, the production rate of nitrogen atoms by cosmic rays at a geomagnetic latitude of 40°N, was obtained from Nicolet (1975) for the height range 35-85 km. Nicolet showed that the dissociation and dissociative ionization of N_2 by cosmic rays yield approximately one nitrogen atom for every ion pair produced by cosmic rays. In this model it is assumed that all the nitrogen atoms produced by cosmic rays are in the ground state (^4S).

Since the model only predicts odd nitrogen components, concentration profiles of the other species had to be provided for both the daytime and nighttime for the height range 35-100 km. This was done by using either observational data or other model data. For almost all the input profiles, points were taken at 5 km intervals and intermediate values were obtained by computer interpolation using an Aitken-Lagrange interpolation scheme. This was also done for photolysis rates J_1, J_7, and J_{58} and production rates r_{31} and r_{59}. In some instances additional points were provided either to resolve a special feature in a profile or because the interpolation scheme needed more points to produce a meaningful curve. All the profiles can be found in Appendix A with values given at 1 km intervals, except for the M profile for which values are given every 0.5 km.

It would have been a more consistent and satisfactory approach to calculate the photolysis and production rates and some of the concentration

profiles rather than to use the results of other modelers or to average many observational profiles. However, since the primary goal was to evaluate a new method for solving a one-dimensional odd nitrogen model, we felt that the calculation of our own profiles would complicate the model and consume too much time for an initial study.

We will now discuss the sources of the profiles. The temperature, N_2, and O_2 profiles for the height range 35-100 km were taken from the Cospar International Reference Atmosphere (1965) at intervals of 1 km, 5 km, and 5 km, respectively. The interpolated values for $[N_2]$ and $[O_2]$ were in excellent agreement with the CIRA values. In this study $[O_2]$ indicates the number density or concentration of the quantity within the brackets, in this case molecular oxygen. The atmospheric number density, [M], was calculated by adding $[N_2]$ and $[O_2]$ for z (altitude) less than 90 km and $[N_2]$, $[O_2]$, and [O] for the height range 90-100 km.

The profiles mentioned thus far are valid for both the daytime and nighttime. However, the following species differ in their daytime and nighttime concentrations. The daytime ozone profile for the height range 35-80 km was taken from Nicolet's (1971) model. This profile compares very favorably with a mid-latitude, mean annual ozone model profile derived by Wu (1974) from daytime measurements. However, Nicolet's values were used in order to keep the major odd oxygen components, O and O_3, compatible since Nicolet's atomic oxygen profile was also used. Model ozone values for 90-100 km were taken from Thomas (1973). The ozone concentration at 85 km is an average of Nicolet's and Thomas' values. The nighttime ozone profile in the upper stratosphere does not differ from the daytime profile; consequently, Nicolet's model values were used for

35-55 km. Above this region (60-100 km) nighttime ozone values were taken from Thomas. His model profile exhibits a dip in the ozone concentration around 80 km which simulates somewhat an actual dip around 75 km in the nighttime ozone concentrations derived from satellite observations (see Wu). The daytime atomic oxygen profile for the 35-85 km region was taken from Nicolet (1971). The O values for 90-100 km were taken at 2 km intervals from the Jacchia (1971) model atmosphere (exospheric temperature = 900°K) and reduced by a factor of 2 in order to make them compatible with observations by Henderson (1971) and by von Zahn et al. (1977). At night [O] drops off rapidly below 85 km and is important only in the lower thermosphere. Values for [O] between 75 and 80 km were taken from Thomas (1973). At 85 km the value is the daytime value from Nicolet, while values for 90-100 km are the daytime Jacchia values. No difference between daytime and nighttime number densities is apparent in this region. Daytime [OH] between 45 and 70 km was obtained from Anderson (1971) who inferred the OH concentrations from dayglow measurements of OH resonance fluorescence. Values for the height ranges 35-40 km and 75-95 km were obtained from the model results of Hunten and Strobel (1974). At night [OH] decreases significantly in the upper stratosphere and in most of the mesosphere so that values were taken from Thomas (1973) only for the height range 60-100 km. Near 80 km the model profile exhibits a rapid increase and then a rapid decrease in [OH]. A daytime electron density profile for the height range 55-100 km at a solar zenith angle of 60° was obtained by averaging the profiles of Mechtly and Smith (1968) obtained over Wallops Island, Virginia. These profiles were found in a paper by Reid (1971). The nighttime electron

density profile was taken from a model by Ogawa and Shimazaki (1975) for the height range 75-80 km and from a model by Keneshea et al. (1970) for 85-100 km. The daytime NO^+ number density for 70-75 km was taken from the observations of Narcisi and Bailey (1965). These observations are illustrated in Fig. 6.16 in a book by McEwan and Phillips (1975). For the height range 80-85 km $[NO^+]$ is an average of the values in the aforementioned Fig. 6.16 and the observational values from Fig. 1 of Narcisi (1973). For 90-95 km $[NO^+]$ is an average of the Narcisi values and the observational values of Johnson (1966) which are illustrated in Fig. 6.15 of McEwan and Phillips. At 100 km the number density is an average of three observational values from Johnson and Narcisi. Two of the values are from Figs. 1 and 5 of the Narcisi paper. Nighttime $[NO^+]$ was taken from a model by Ogawa and Shimazaki (1975) for 75-80 km and from a model by Keneshea et al. (1970) for 85-100 km.

Mid-latitude diurnal mean values for $[O(^1D)]$ were obtained from the extended model of Prinn et al. (1975) and multiplied by 2 to obtain daytime values for the height range 35-50 km. At night $O(^1D)$ effectively disappears in this region. The daytime nitrous oxide profile was determined from the balloon and rocket data of Ehhalt et al. (1974, 1975). Their values at 29.5, 32.0, 44.5, and 50 km were graphed, and then N_2O concentration values were taken at 5 km intervals from 35-50 km. Since reaction 54 becomes unimportant at night because of the disappearance of $O(^1D)$, the inclusion of the nighttime N_2O profile is unnecessary. The daytime $O_2(^1\Delta_g)$ profile for the height range 50-95 km was obtained by averaging the observational profiles in Fig. 2 of Llewellyn et al. (1973). At night $[O_2(^1\Delta_g)]$ decreases considerably throughout the 50-95 km height range, thus making reaction 4 unimportant in this model. For this reason

the nighttime $O_2(^1\Delta_g)$ profile was not included. The daytime O_2^+ profile was taken from the same sources as the NO^+ profile. The value at 75 km was from Fig. 6.16. The value at 80 km is an average of values from Figs. 6.16 and 1. At 85 km the value is from Fig. 1. For 90-95 km the number densities are averages of values from Figs. 6.15 and 1. At 100 km, the value is an average of values from Figs. 6.15, 1, and 5. The nighttime profile is not included since $[O_2^+]$ decreases appreciably thus making reaction 39 unimportant. The daytime N_2^+ profile for 90-100 km was determined by averaging Johnson's (1966) model values in Strobel et al. (1970) and the model results of Ogawa and Shimazaki (1975). The nighttime profile is not included since $[N_2^+]$ decreases appreciably thus making reaction 34 unimportant. Finally, the daytime O^+ profile for 95-100 km was taken from Ogawa and Shimazaki's model. The nighttime profile is not included since $[O^+]$ decreases considerably thus making reaction 35 unnecessary.

Since vertical transport in the model is described by diffusion, the appropriate eddy and molecular diffusion coefficients had to be prescribed. The profiles that were used can be seen in Fig. 1. One of the profiles chosen is that recommended by Hunten (1975), and the model using it will be referred to as model AL. This K profile increases exponentially to a value of 1×10^5 cm^2 sec^{-1} at 50 km with a scale height, H_K, of 9.43 km, to a value of 1×10^6 cm^2 sec^{-1} at 80 km with H_K = 13 km, and then remains constant to 100 km. A modification of this profile above 80 km, hereafter referred to as model AH, allows K to increase exponentially to 4.5×10^6 cm^2 sec^{-1} at 100 km with H_K = 13.3 km. This "high" K comes from Colegrove et al. (1966). A profile with lower

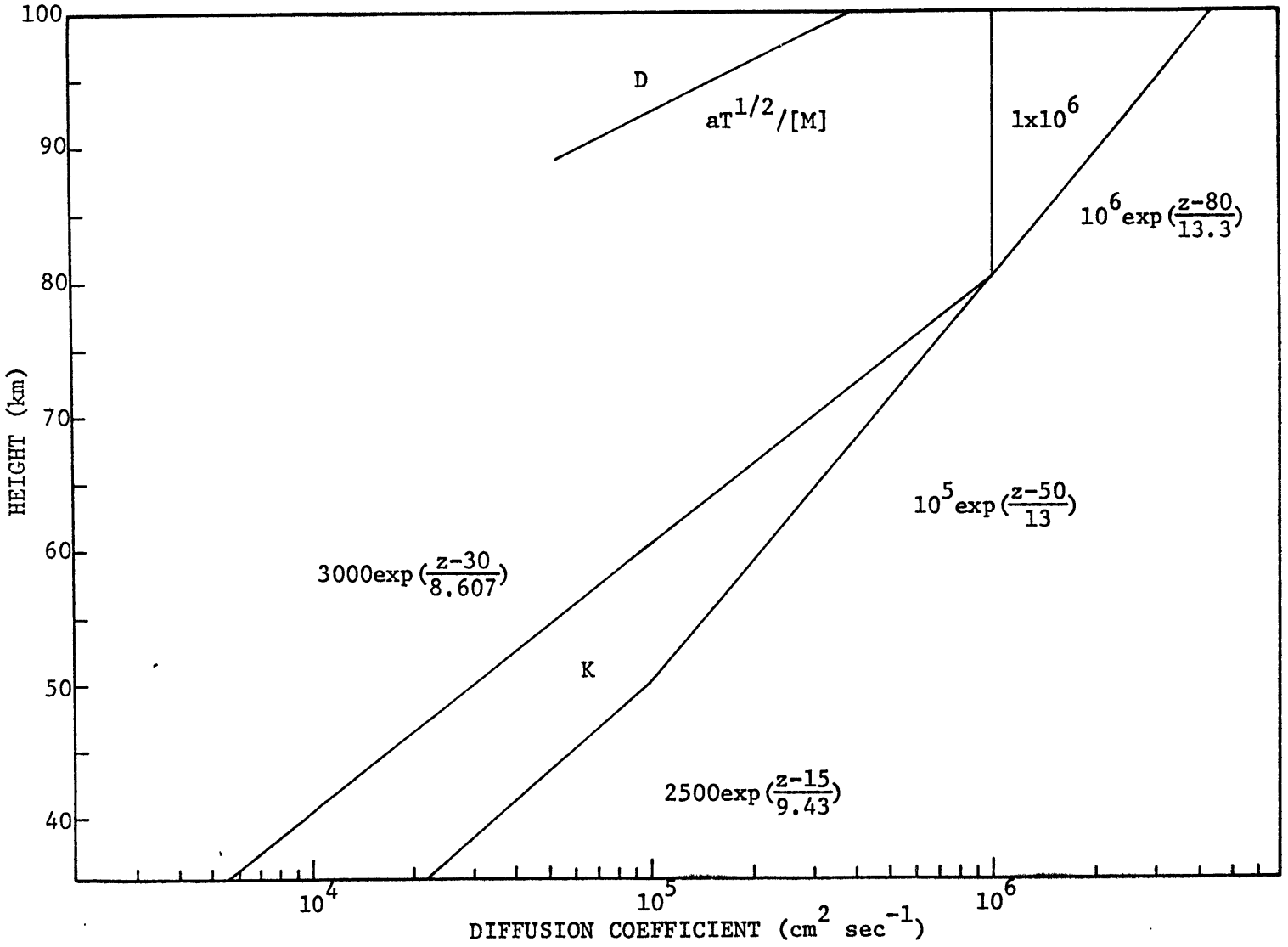
100
90
80
70
60
50
40
HEIGHT (km)
D
$aT^{1/2}/[M]$
$1x10^6$
$10^6 exp(\frac{z-80}{13.3})$
$10^5 exp(\frac{z-50}{13})$
$3000exp(\frac{z-30}{8.607})$
K
$2500exp(\frac{z-15}{9.43})$
10^4
10^5
10^6
DIFFUSION COEFFICIENT (cm^2 sec^{-1})

Figure 1

K values in the upper stratosphere and the mesosphere was also chosen for investigation. This profile, hereafter referred to as model BL, is a slight alteration of a profile used by Hunten and Strobel (1974). The profile increases exponentially to a value of 1×10^6 cm^2 sec^{-1} at 80 km (H_K = 8.607 km) and then remains constant to 100 km. Again, a modification of this profile above 80 km, hereafter referred to as model BH, allows K to increase exponentially to 4.5×10^6 cm^2 sec^{-1} at 100 km with H_K = 13.3 km. The molecular diffusion coefficient, D, was approximated by an expression obtained from Strobel et al. (1970) with $a = 2.98 \times 10^{17}$ cm^{-1} sec^{-1} $(°K)^{-1/2}$ for nitric oxide. In the 90-100 km region the number densities of all other odd nitrogen constituents are much less than [NO] so that molecular diffusion of other odd nitrogen species did not have to be considered in this model.

Since the model requires upper and lower boundary conditions for its solution, actual observational values were chosen for those boundary conditions. At the lower boundary (35 km) we used the average total measured NO_y (= NO + NO_2 + HNO_3) from Fig. 4 of a review paper by Ridley (1977). The value for the number density was 1.68×10^9 cm^{-3}. At the upper boundary (100 km) an average of the NO measurements of Barth (1966) and Meira (1971) was calculated. The values were taken from Meira's Fig. IV-8. The number density obtained was 7.4×10^7 cm^{-3}. It was assumed that the boundary conditions would not vary diurnally. More will be said later about this assumption.

3. Model Formulation

This section will deal with the formulation of the equations for the odd nitrogen model. The odd nitrogen components we will be concerned with are $N(^4S)$, $N(^2D)$, NO, NO_2, and HNO_3. In order to solve our one-dimensional aeronomical problem, we need to specify a continuity equations for i constituents

$$\frac{\partial n_i}{\partial t} + \frac{\partial \phi_i}{\partial z} = p_i - l_i \tag{1}$$

where n_i is the number density or concentration of the ith constituent, t is time, ϕ_i is the flux of i, z is the altitude, and p_i and l_i are the chemical production and loss rates per unit volume. In our case i refers to total odd nitrogen. The vertical flux, ϕ_i, is described by the standard mixing length approximation

$$\phi_{ON} = -K[M] \frac{\partial f_{ON}}{\partial z} \tag{2}$$

where K is the eddy diffusion coefficient, [M] is the atmospheric number density, and f_{ON} is the number mixing ratio of ON. For the height range 90-100 km the effect of molecular diffusion is included

$$\phi_{ON} = -(K + D_{ON})[M] \frac{\partial f_{ON}}{\partial z} \tag{3}$$

where D_{ON} is the molecular diffusion coefficient for nitric oxide, as mentioned previously. The addition of molecular diffusion in this fashion

is a valid approximation if the scale height of the diffusing species is approximately equal to the scale height of the background atmosphere (see Equation 3, Hunten and Strobel, 1974); this is the case here. With the continuity and flux equations specified, and with the boundary conditions provided previously, all that remains is a specification of the production and loss rates before the numerical technique can be applied. An initial condition is also needed, but this is no problem.

However, before discussing the production and loss terms, a few words should be said about the interaction between chemistry and dynamics in this model. One of the simplest ways to examine this question is to compare the chemical and dynamical time constants for the loss and diffusion, respectively, of odd nitrogen. The chemical time constant, τ_c, is governed by reaction 2 with reactions 14_a, 14_b, and 14_c being important in those regions where NO_2 is a significant fraction of the total odd nitrogen. The dynamical time constant, τ_K, is H^2/K where H is the scale height of the background atmosphere. After examining the time constants in Table 2 for models AL and AH for both the daytime and nighttime, we can make several observations. Since the dynamical time constants are on the order of or less than the chemical time constants, transport by eddy diffusion cannot be neglected. No diurnal variation in odd nitrogen will be evident in the upper stratosphere and through most of the mesosphere since the dynamical and chemical time constants are much longer than a day. Some diurnal variation in the upper mesosphere and lower thermosphere can be expected since the dynamical and chemical time constants are on the order of one day. Finally, because the dynamical time constants are much smaller than the chemical ones, transport of odd

Table 2. A comparison of chemical and dynamical time constants for models AL and AH ("high" K profile). Time constants have units sec.

z (km)	τ_K(AL)	τ_c(AL)*	τ_c(AL)**	τ_K(AH)	τ_c(AH)*	τ_c(AH)**
35	2.4×10^{7}	1.9×10^{9}	6.2×10^{10}	2.4×10^{7}	1.9×10^{9}	6.2×10^{10}
40	1.6×10^{7}	1.7×10^{8}	7.0×10^{10}	1.6×10^{7}	1.7×10^{8}	7.0×10^{10}
45	1.0×10^{7}	3.4×10^{7}	5.9×10^{10}	1.0×10^{7}	3.3×10^{7}	5.9×10^{10}
50	6.5×10^{6}	1.8×10^{7}	6.1×10^{10}	6.5×10^{6}	1.8×10^{7}	6.1×10^{10}
55	3.9×10^{6}	7.2×10^{6}	3.2×10^{10}	3.9×10^{6}	6.8×10^{6}	3.2×10^{10}
60	2.4×10^{6}	3.3×10^{6}	2.1×10^{10}	2.4×10^{6}	2.9×10^{6}	2.1×10^{10}
65	1.5×10^{6}	1.6×10^{6}	6.0×10^{9}	1.5×10^{6}	1.2×10^{6}	6.1×10^{9}
70	9.0×10^{5}	7.8×10^{5}	2.3×10^{9}	9.0×10^{5}	4.9×10^{5}	2.5×10^{9}
75	5.4×10^{5}	4.1×10^{5}	8.6×10^{8}	5.4×10^{5}	2.0×10^{5}	1.5×10^{9}
80	3.1×10^{5}	1.9×10^{5}	4.3×10^{9}	3.1×10^{5}	1.0×10^{5}	6.4×10^{9}
85	3.1×10^{5}	7.6×10^{4}	2.0×10^{8}	2.1×10^{5}	5.9×10^{4}	7.8×10^{8}
90	$3.2(3.0)\times10^{5+}$	4.6×10^{4}	1.4×10^{8}	$1.5(1.5)\times10^{5+}$	5.0×10^{4}	5.2×10^{8}
95	$3.7(3.2)\times10^{5+}$	3.7×10^{4}	1.1×10^{8}	$1.2(1.1)\times10^{5+}$	4.3×10^{4}	2.1×10^{8}
100	$4.2(3.0)\times10^{5+}$	3.3×10^{4}	3.6×10^{7}	$9.3(8.5)\times10^{4+}$	3.3×10^{4}	3.6×10^{7}

* Daytime values.

** Nighttime values.

\+ Values in parentheses are $H^2/(K + D_{ON})$.

nitrogen at night is very important while chemical loss is insignificant.

Since the numerical method involves integrating through two different regimes, the daytime and the nighttime, each 12 hours long, we will likewise separate our discussion into one dealing with the daytime chemistry and one with the nighttime chemistry. First, we will discuss the daytime regime, which we will divide into three separate regions: the upper stratosphere, from 35-50 km; the mesosphere, from 50-80 km; and the lower thermosphere, from 80-100 km. The stratopause is at 50 km and the mesopause at 80 km. In the upper stratosphere the primary odd nitrogen constituents are NO and NO_2. HNO_3 is included for the sake of completeness. NO and NO_2 are in photochemical steady-state during the daytime since their chemical time constants for loss are much shorter than 12 hours and much shorter than the time constants for eddy transport. Assuming photochemical steady-state for NO_2, we can write the following relation for the interconversion of one species into another

$$[NO_2] = \alpha [NO] \tag{4}$$

where $$\alpha = \left(k_{10}[O_3] + k_{11}[O][M] + k_{12}[O]\right) / \left(J_{13} + k_{15}[O]\right)$$

Equation 4 is actually valid for the entire height range 35-100 km since τ_c = 111 sec for NO_2. HNO_3 is also assumed to be in photochemical steady-state although the approximation is not as good since the chemical time constant is on the order of 9 hours at 35 km and 2 hours at 50 km. The following relation can be written

$$[HNO_3] = \beta [NO_2]$$

(5)

where $\beta = k_{55}[OH][NO_2][M] / (k_{56}[O] + k_{57}[OH] + J_{58})$

We can now define odd nitrogen in the following manner

$$[ON] \simeq [NO] + [NO_2] + [HNO_3]$$

(6)

Using equations (4) and (5) we obtain

$$[NO] = \gamma [ON]$$

(7)

where $\gamma = 1 / (1 + \alpha + \beta\alpha)$

We are now ready to write an expression for the production and loss rates of odd nitrogen:

$$P_{ON} - L_{ON} = 2k_{54}[N_2O][O(^1D)] + r_{59} - 2[N(^4S)](k_2[NO] + (k_{14a} + k_{14b} + k_{14c})[NO_2])$$

(8)

Equation (8) can be written in terms of ON by using Equations (4) and (7)

(with $k_{14abc} = k_{14a} + k_{14b} + k_{14c}$):

$$p_{ON} - l_{ON} = 2\left(k_{54}[N_2O][O(^1D)] - [N(^4S)]\,\gamma\,[ON]\left(k_2 + k_{14abc}\alpha\right)\right) + r_{59}$$

(9)

The only unknown that remains to be specified is $[N(^4S)]$. Since it is in photochemical steady-state we can write (using Equation (7))

$$[N(^4S)] = \left(J_7\gamma[ON] + r_{59}\right)\Big/\left(\gamma[ON]\left(k_2 + \alpha k_{14}\right) + k_3[O_2] + k_5[O_3]\right)$$

(10)

With Equations (9) and (10) given, the description of the odd nitrogen chemistry for the height range 35-50 km is complete.

In the daytime mesosphere odd nitrogen consists almost entirely of NO. NO_2 and HNO_3, determined by using α and β, respectively, are very small fractions of the total ON. The largest constituent other than NO is ground state atomic nitrogen, $N(^4S)$, which at its closest, comes within approximately 2.5 percent of ON (in model AL at 79 km). Therefore, we can assume

$$[ON] \simeq [NO]$$

(11)

The expression for the production and loss rates of odd nitrogen is (using Equation (11))

$$p_{ON} - l_{ON} = -2k_2[N(^4S)][ON] \tag{12}$$

$N(^4S)$ is assumed to be in photochemical steady-state with the longest chemical time constant calculated to be approximately one hour (model AL). We can write (using Equation (11))

$$[N(^4S)] = J_7[ON]/(k_2[ON] + k_3[O_2] + k_4[O_2(^1\Delta_g)] + k_5[O_3] + k_{16}[OH]) \tag{13}$$

Equations (12) and (13) describe the odd nitrogen chemistry for the height range 51-79 km.

In the daytime lower thermosphere odd nitrogen again consists almost entirely of NO so that Equation (11) applies. The largest constituent other than NO is again $N(^4S)$ which comes, at its closest, within approximately 10 percent of ON (in model AL at 87 km). The expression for the production and loss rates of odd nitrogen is (using Equation (11))

$$p_{ON} - l_{ON} = 2(J_1[N_2] + r_{31} - k_2[N(^4S)][ON]) + k_{34}[N_2^+][O] + k_{35}[O^+][N_2] \tag{14}$$

$N(^4S)$ is again assumed to be in photochemical steady-state with the longest chemical time constant calculated to be approximately two hours (model AL). We can write (using Equation (11))

$$[N(^4S)] = (2J_1[N_2] + J_7[ON] + [N(^2D)](k_{17}[N_2] + k_{20}[O]) + r_{31} + k_{32}(1-A)[NO^+][e^-] + k_{35}[O^+][N_2])/(k_2[ON] + k_3[O_2] + k_4[O_2(^1\Delta_g)] + k_5[O_3] + k_{16}[OH] + k_{25}[O] + k_{39}[O_2^+])$$

(15)

In order to calculate $[N(^4S)]$, we need an expression for atomic nitrogen in the excited state (^2D). $N(^2D)$ is in photochemical steady-state in this region since it has extremely short chemical time constants. Therefore, we can write

$$[N(^2D)] = (r_{31} + k_{32}(A)[NO^+][e^-] + k_{34}[N_2^+][O])/(k_9[O_2] + k_{17}[N_2] + k_{20}[O])$$

(16)

Equations (14), (15), and (16) end the presentation of the daytime odd nitrogen chemistry necessary in the formulation of the model.

In the nighttime regime the chemistry undergoes a significant change since the reactions driven by sunlight are no longer important. Nitric

oxide is rapidly converted to NO_2 via reaction 10 up to a height of approximately 62 km where the [NO] is reduced to about 6 percent of its initial value in 12 hours. NO can therefore be considered in photochemical steady-state below this height, and we can write the following expression

$$[NO] = [N(^4S)]\left(k_3[O_2] + k_5[O_3] + k_{16}[OH] + 2k_{14d}[ON]\right) \Big/ k_{10}[O_3] \tag{17}$$

The concentration of odd nitrogen is given by

$$[ON] \simeq [NO_2] \tag{18}$$

since NO_2 is the primary species. Nitric acid is inconsequential in this region at night because of a lack of significant production mechanisms. Nitrogen trioxide is expected to have a strong diurnal variation with maximum concentrations during the night. However, the reaction of NO_2 with O_3 is not fast enough to produce concentrations of NO_3 that are a sizable fraction of the total odd nitrogen. Therefore, we have not included NO_3 in the model. The concentration of $N(^4S)$ is much smaller at night in the entire height range (35-100 km) because the main source of $N(^4S)$, reaction 7, is no longer operating. The primary source of $N(^4S)$ is now the dissociation of molecular nitrogen by cosmic rays. $N(^4S)$ is assumed to be in photochemical steady-state with the longest time constant calculated to be approximately 2 hours (model AL). The expressions for $N(^4S)$

will be presented later in this discussion.

In the height range 62-72 km, odd nitrogen is given by

$$[ON] \simeq [NO] + [NO_2] \tag{19}$$

with [NO] increasing and $[NO_2]$ decreasing upwards. At 72 km [NO] is reduced to 95 percent of its initial value in 12 hours by reaction 10. Above 72 km odd nitrogen is given by

$$[ON] \simeq [NO] \tag{20}$$

since reaction 10 is no longer an important loss mechanism for NO. One point should be made about the limiting heights 62 and 72 km. These values are not rigid since they are based on time constant considerations. A criterion of approximately 5 percent was used. Slightly more conservative heights were used in the actual model calculations. Finally, NO_2 is in photochemical steady-state above approximately 79 km since reaction 15 is so rapid in converting NO_2 to NO. The expression for NO_2 is (using Equation (20))

$$[NO_2] = [ON]\left(k_{10}[O_3] + k_{11}[O][M] + k_{12}[O]\right) / k_{15}[O] \tag{21}$$

The expressions that were used in the model for the nighttime production and loss rates of odd nitrogen can now be presented. For the height range 35-60 km the expression is (using Equation (18))

$$p_{ON} - l_{ON} = r_{59} - 2(k_{14abc})[N(^4S)][ON] \tag{22}$$

The $N(^4S)$ concentration is given by (using Equation (18))

$$[N(^4S)] = r_{59} / (k_3[O_2] + k_5[O_3] + k_{14}[ON]) \tag{23}$$

For the height range 61–78 km the production and loss rates are

$$p_{ON} - l_{ON} = r_{59} - 2[N(^4S)](k_2[NO] + k_{14abc}[NO_2]) \tag{24}$$

By using Equation (19) and recognizing that k_2 is approximately equal to k_{14abc}, we can write Equation (24) as

$$p_{ON} - l_{ON} = r_{59} - 2k_2[N(^4S)][ON] \tag{25}$$

$[N(^4S)]$ is given by (using Equation (19))

$$[N(^4S)] = (r_{59} + k_{32}(1-A)[NO^+][e^-]) / (k_2[ON] + k_3[O_2] + k_5[O_3] + k_{16}[OH]) \tag{26}$$

For the height range 79–100 km the production and loss rates are (using Equation (20))

$$p_{ON} - l_{ON} = r_{59} - 2 k_2 [N(^4S)][ON] \tag{27}$$

$[N(^4S)]$ is given by (using Equation (20))

$$[N(^4S)] = \left(r_{59} + k_{32}(1-A)[NO^+][e^-] + [N(^2D)]\left(k_{17}[N_2] + k_{20}[O]\right)\right) / \left(k_2[ON] + k_3[O_2] + k_5[O_3] + k_{16}[OH] + k_{25}[O]\right) \tag{28}$$

$N(^2D)$ is in photochemical steady-state since it has extremely short chemical time constants. Therefore, we can write

$$[N(^2D)] = k_{32}(A)[NO^+][e^-] \Big/ \left(k_9[O_2] + k_{17}[N_2] + k_{20}[O]\right) \tag{29}$$

Equations (27), (28), and (29) end the presentation of the nighttime odd nitrogen chemistry necessary in the formulation of the model.

4. Numerical Technique and Results

This section will discuss the numerical techniques used and the results obtained, from a numerical standpoint. In order to perform a time integration of the continuity equation for odd nitrogen, Lorenz's (1971) simple N-cycle scheme was used with N = 4. The time steps varied from $\Delta t = 0.1$ hr to $\Delta t = 0.3$ hr, the choice of which appeared to depend upon the K profile in the upper thermosphere. The fundamental time increment is actually $N\Delta t$ since the predicted values were always taken after the fourth cycle was completed. We will, however, refer to Δt as our time step. Central differences were used for the finite difference equivalents of the spatial derivatives. The vertical resolution of the model was 1 km ($\Delta z = 1$ km).

In order to apply the N-cycle scheme, Equation (1) was first put in the following form

$$\frac{\partial f_{ON}}{\partial t} = \frac{1}{[M]}\left[\frac{\partial}{\partial z}\left(K[M]\frac{\partial f_{ON}}{\partial z}\right) + (p_{ON} - l_{ON})\right] \tag{30}$$

From this point on the terms in the brackets will be referred to as the flux convergence, conv, on the left, and the chemical production and loss rate, chem, on the right. If conv is positive, the flux of odd nitrogen converges; if negative, the flux diverges. If chem is positive, there is a net production of odd nitrogen; if negative, there is a net loss. The convergence term was written in finite difference form as follows

$$\left[\frac{\partial}{\partial z}\left(K[M]\frac{\partial f_{ON}}{\partial z}\right)\right]_k = \left[(K[M])_{k+\frac{1}{2}} f_{ON_{k+1}} - [(K[M])_{k+\frac{1}{2}} + (K[M])_{k-\frac{1}{2}}] f_{ON_k} + (K[M])_{k-\frac{1}{2}} f_{ON_{k-1}}\right] / (\Delta z)^2$$

(31)

where k refers to levels in the model at 1 km intervals beginning at 35 km and ending at 100 km. The intermediate levels (k ± 1/2) lie halfway between the levels at which values were calculated for f_{ON}. The fluxes of odd nitrogen were calculated at these intermediate levels with the following finite difference form

$$\left[-K[M]\frac{\partial f_{ON}}{\partial z}\right]_{k+\frac{1}{2}} = -(K[M])_{k+\frac{1}{2}} \frac{f_{ON_{k+1}} - f_{ON_k}}{\Delta z}$$

(32)

For the height range 90-100 km, K was replaced by $K + D_{ON}$. With the right-hand side of Equation (30) in finite difference form, values for this quantity were calculated at every level from 36-99 km at each time step in the N-cycle scheme, and then were used to calculate new values for f_{ON} at every level. The f_{ON} values were taken after the fourth cycle was completed.

Before the time integration of Equation (30) could begin, the boundary conditions at 35 and 100 km and an initial profile for f_{ON} had to be provided. The mixing ratio equivalents of the odd nitrogen concentration values discussed in the Input Data section were used for the boundary conditions. The initial profile used was the mixing ratio equivalent of the following expression

$$[ON] = \exp(-4.80382 \times 10^{-2} z + 22.9234) \tag{33}$$

The time integration was started using daytime chemistry and was run for a period of 12 model hours. The f_{ON} values computed at the end of that period were then used as initial values for the nighttime integration which proceeded for a period of 12 model hours. The f_{ON} values at night's end were then used as input values for the daytime integration; this cycle was repeated until equilibrium was attained. No discernible numerical problems were encountered in switching from one regime to another. This behavior is consistent with the dynamical and chemical time constants exhibited in Table 2 which imply that no large diurnal variation in odd nitrogen is to be expected throughout the entire height range of the model.

The following criterion was used to determine if an equilibrium state had been achieved. Since the dynamical and chemical time constants are largest in the upper stratosphere and are much greater than a day, the time necessary to reach equilibrium for the entire model will be determined by the chemistry and dynamics in the upper stratosphere.

Here an actual steady-state solution is expected (and was obtained); therefore, the sum of the average chemistry and average flux convergence terms should be equal to zero. The method was to compute (at every point from 36-50 km) a ratio of the average of the daytime and nighttime flux convergences to the average of the daytime and nighttime chemical production and loss terms. The absolute value of this ratio should be equal to 1 at steady-state. However, since we are dealing with a numerical model, this ratio will be close to 1. In the upper mesosphere and lower thermosphere this ratio should be significantly different from 1 since a pseudo steady-state solution is expected. These statements are confirmed by the equilibrium results shown in Table 3 for model AH and Table 4 for model AL. Illustrated are the daytime and nighttime flux convergences and chemical production and loss rates along with the ratios calculated using these terms. The chemistry and convergence values were taken at the end of the daytime and nighttime integrations. It is evident that in the upper stratosphere and in most of the mesosphere the absolute value of the ratio is close to 1, while in the upper mesosphere and lower thermosphere it is appreciably greater than 1. After the absolute values of the ratios in the upper stratosphere were calculated, the absolute values of the differences between these ratios and 1 were calculated and compared with a set value which we shall call crit. If the differences were less than or equal to crit for the entire height range, then equilibrium was attained. This condition had to be met for a period of 5 consecutive days in order for the model to stop integrating. A further check was performed by determining if the diurnally integrated flux into the top of the model was balanced by the sum of the diurnally and

Table 3. A comparison of model AH (A = 0.5) daytime and nighttime flux convergences and chemical production and loss rates. The absolute value of the ratio of the average of the convergences to the average of the chemical rates is also presented. Rates and convergences have units cm^{-3} sec^{-1}.

	DAYTIME		NIGHTTIME		
z(km)	conv	chem	conv	chem	|ratio|
36	-3.42×10^{1}	6.54×10^{1}	-3.07×10^{1}	7.54×10^{-1}	0.982
39	-1.50×10^{1}	3.01×10^{1}	-1.50×10^{1}	4.92×10^{-1}	0.979
42	-3.92×10^{0}	7.68×10^{0}	-3.98×10^{0}	3.29×10^{-1}	0.986
45	1.98×10^{0}	-4.44×10^{0}	1.97×10^{0}	2.24×10^{-1}	0.937
48	3.93×10^{0}	-8.01×10^{0}	3.93×10^{0}	1.52×10^{-1}	1.001
51	4.15×10^{0}	-8.29×10^{0}	4.02×10^{0}	1.04×10^{-1}	0.999
54	4.41×10^{0}	-8.92×10^{0}	4.44×10^{0}	7.44×10^{-2}	1.001
57	4.58×10^{0}	-9.20×10^{0}	4.62×10^{0}	4.73×10^{-2}	1.005
60	4.72×10^{0}	-9.45×10^{0}	4.80×10^{0}	3.27×10^{-2}	1.011
63	5.09×10^{0}	-1.02×10^{1}	5.29×10^{0}	2.34×10^{-2}	1.014
66	5.99×10^{0}	-1.22×10^{1}	6.47×10^{0}	1.62×10^{-2}	1.023
69	7.97×10^{0}	-1.66×10^{1}	9.27×10^{0}	9.27×10^{-3}	1.039
72	1.26×10^{1}	-2.64×10^{1}	1.56×10^{1}	2.74×10^{-3}	1.067
75	2.13×10^{1}	-4.47×10^{1}	2.81×10^{1}	-1.77×10^{-3}	1.106
78	3.66×10^{1}	-7.73×10^{1}	5.24×10^{1}	-1.59×10^{-3}	1.151
81	5.90×10^{1}	-1.32×10^{2}	1.00×10^{2}	-2.11×10^{-3}	1.210
84	1.11×10^{2}	-2.40×10^{2}	1.88×10^{2}	-1.89×10^{-2}	1.244
87	1.80×10^{2}	-3.96×10^{2}	3.27×10^{2}	-5.25×10^{-2}	1.278
90	2.78×10^{2}	-5.65×10^{2}	4.51×10^{2}	-8.99×10^{-2}	1.290
93	4.86×10^{2}	-7.41×10^{2}	4.14×10^{2}	-1.87×10^{-1}	1.215
96	8.57×10^{2}	-9.99×10^{2}	2.36×10^{2}	-4.56×10^{-1}	1.093
99	1.44×10^{3}	-1.46×10^{3}	4.80×10^{1}	-1.36×10^{0}	1.013

Table 4. A comparison of model AL (A = 0.5) daytime and nighttime flux convergences and chemical production and loss rates. The absolute value of the ratio of the average of the convergences to the average of the chemical rates is also presented. Rates and convergences have units cm^{-3} sec^{-1}.

	DAYTIME		NIGHTTIME		
z(km)	conv	chem	conv	chem	|ratio|
36	-3.46×10^{1}	6.54×10^{1}	-3.12×10^{1}	7.54×10^{-1}	0.994
39	-1.53×10^{1}	3.01×10^{1}	-1.52×10^{1}	4.92×10^{-1}	0.996
42	-4.04×10^{0}	7.78×10^{0}	-4.01×10^{0}	3.29×10^{-1}	0.993
45	2.00×10^{0}	-4.22×10^{0}	1.98×10^{0}	2.24×10^{-1}	0.998
48	3.81×10^{0}	-7.68×10^{0}	3.74×10^{0}	1.52×10^{-1}	1.003
51	3.92×10^{0}	-7.83×10^{0}	3.83×10^{0}	1.04×10^{-1}	1.004
54	4.05×10^{0}	-8.14×10^{0}	4.04×10^{0}	7.45×10^{-2}	1.003
57	3.97×10^{0}	-7.95×10^{0}	3.98×10^{0}	4.74×10^{-2}	1.005
60	3.73×10^{0}	-7.47×10^{0}	3.76×10^{0}	3.28×10^{-2}	1.008
63	3.49×10^{0}	-6.99×10^{0}	3.53×10^{0}	2.38×10^{-2}	1.009
66	3.32×10^{0}	-6.64×10^{0}	3.40×10^{0}	1.68×10^{-2}	1.015
69	3.32×10^{0}	-6.70×10^{0}	3.52×10^{0}	1.05×10^{-2}	1.023
72	3.74×10^{0}	-7.60×10^{0}	4.13×10^{0}	4.97×10^{-3}	1.035
75	4.57×10^{0}	-9.23×10^{0}	5.14×10^{0}	6.03×10^{-4}	1.052
78	6.60×10^{0}	-1.19×10^{1}	6.04×10^{0}	2.21×10^{-4}	1.060
81	3.38×10^{0}	-1.12×10^{1}	9.46×10^{0}	-1.52×10^{-4}	1.146
84	1.06×10^{1}	-2.74×10^{1}	2.29×10^{1}	-1.33×10^{-2}	1.219
87	3.67×10^{1}	-7.33×10^{1}	5.36×10^{1}	-4.32×10^{-2}	1.231
90	7.36×10^{1}	-1.55×10^{2}	1.20×10^{2}	-8.32×10^{-2}	1.252
93	1.31×10^{2}	-2.87×10^{2}	2.41×10^{2}	-1.81×10^{-1}	1.293
96	3.62×10^{2}	-5.43×10^{2}	2.94×10^{2}	-4.52×10^{-1}	1.206
99	1.19×10^{3}	-1.24×10^{3}	9.00×10^{1}	-1.36×10^{0}	1.028

spatially integrated chemical production and loss in the model and the diurnally integrated flux out of the bottom of the model. In other words,

$$\sum_{24\,hr} \phi_{ON}\Big|_{z=99.5\,km} = \left[\sum_{24\,hr}\sum_{z=36\,km}^{99\,km} chem_{ON}\right]\Delta z + \sum_{24\,hr} \phi_{ON}\Big|_{z=35.5\,km}$$

(33)

This check was applied to the final day of a model run.

The results obtained will now be discussed from the standpoint of the equilibrium criteria chosen. Three runs were made with the model AL K profile with parameter A being varied from 0.0 to 1.0. For A = 0.5 the model reached equilibrium in 708 days with crit = .02 and Δt = 0.3 hr. A crit value of .01 did not allow the model to reach equilibrium. Actual computer execution time (not including input-output time) was 0.58 min. The left- and right-hand sides of Equation (33) came within 1.56 percent of each other. The other two runs were similar. Three runs were also made with the model AH K profile with A varied from 0.0 to 1.0. For A = 0.5 the model reached equilibrium in 573 days with crit = .08 and Δt = 0.1 hr. A crit value of .05 did not allow the model to reach equilibrium. Execution time was 1.42 min, and the balance in Equation (33) was within 1.15 percent. The other two runs were again similar. Model BL was run with A = 0.5. It reached equilibrium in 1390 days with crit = .04 and Δt = 0.3 hr. A crit value of .02 did not allow equilibrium to be reached. Execution time was

1.12 min, and the balance in Equation (33) was within 1.56 percent. Model BH (A = 0.5) presented a problem. With a crit value of less than approximately .95, the model would not stop integrating. With a value greater than that, the model would stop in a very short period of time, but it would not be in equilibrium. In order to obtain some results, the model was run for 738 days (execution time was 1.76 min) with crit = .01 and Δt = 0.1 hr. Even though the model was integrated for approximately half the number of days that model BL was integrated, the daytime stratospheric [ON] values from both models differed by only 1-5 percent with the differences increasing upward from the bottom of the model. Also, the balance in Equation (33) was within 0.98 percent. The values computed for the ratio of the convergence to the chemical production and loss were examined to determine why the crit value had to be set so high in order to stop the model. The ratios ranged from 1.003 to 2.52 at 43 km. This high value occurred at a point in the daytime regime where conv and chem change signs in going from 43-44 km. After checking the results of the other runs, we found that the highest or lowest value for this ratio in the stratosphere occurred at or near this area of sign change which remained the same in all the models. Therefore, it is not surprising that the values for the ratios did not behave smoothly in this region. Finally, the values chosen for crit were not very critical. In other words, a point was reached where lower values for crit would not result in significantly different odd nitrogen concentrations in the upper stratosphere.

We will conclude this section by discussing the time steps chosen for integrating the model. An attempt was made to select the largest

time step possible in order to minimize the computer time needed and to insure that an equilibrium state could be attained in a reasonable amount of running time. Therefore, several time steps were tried in each model in order to achieve this goal. For model AH a time step of 0.1 hr was found to meet the criteria while a time step of 0.15 hr resulted in the model becoming unstable. For model AL a Δt of 0.3 hr was adequate with a time step of 0.4 hr resulting in instability. Since the only difference in the two models is the eddy diffusion coefficient in the lower thermosphere, it was suspected that a larger K necessitated a smaller time step. This was confirmed by running a model in which the largest K was 3×10^5 cm^2 sec^{-1} in the lower thermosphere. A time step of 0.6 hr was suitable while a time step of 1 hr resulted in instability. It appears that the numerical scheme requires relatively small time steps to resolve relatively large fluxes of odd nitrogen.

5. Chemical and Dynamical Results

In this section we will illustrate the results of the model and augment some of the previous discussions in order to improve our understanding of the odd nitrogen chemistry and dynamics. The results of all the runs can be found in Appendix B in tabular form. If the reader wishes to compare these results with the results of other one-dimensional odd nitrogen models, the following sources can be consulted: Norton and Barth (1970), Strobel et al. (1970), Strobel (1971a, 1971b, 1972a, 1972b), Brasseur and Nicolet (1973), McConnell and McElroy (1973), Oran et al. (1975), and Ogawa and Shimazaki (1975).

The results for [ON] for the model AL and model AH K profiles with A = 0.5 can be seen in Figure 2. The daytime and nighttime profiles were taken at the end of the daytime and nighttime integrations. The average profile was calculated by averaging the daytime and nighttime profiles. Such an average profile will be used to portray the results of different eddy diffusion coefficient models in many of the remaining illustrations. We will assume that our average [ON] profile in the upper mesosphere and lower thermosphere is representative not only of the diurnally averaged ON concentration profile but also of the daytime and nighttime average ON concentration profiles. We can justify this assumption by referring to Figures 3 and 4 which present the ON concentrations as a function of time for models AL and AH. These values were taken from the last two days of each model; the values at time 0 hr are the initial values for the daytime integration. It is clear from these diagrams that the daytime and nighttime concentrations are quite symmetric and decrease and

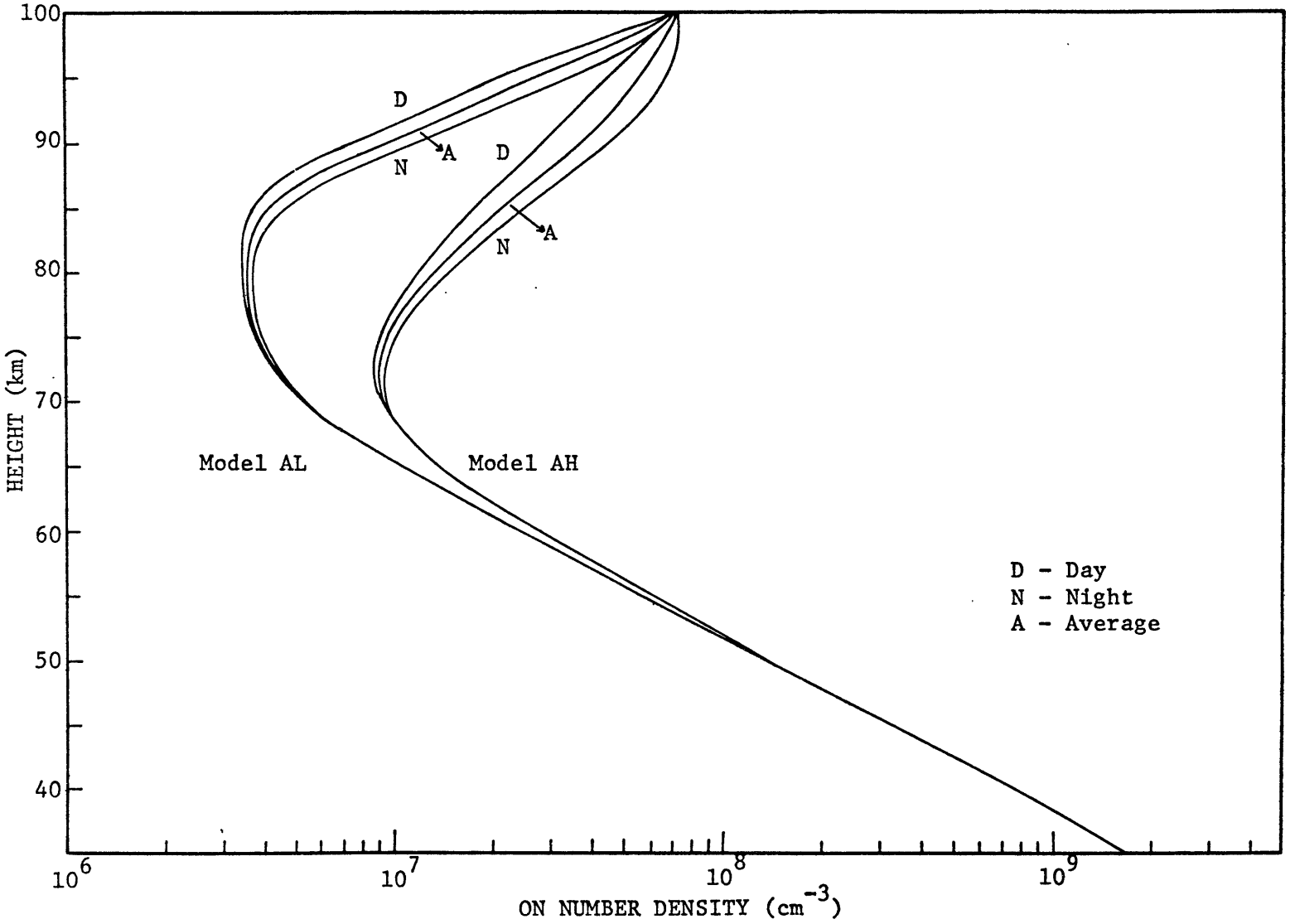
100
90
80
70
60
50
40
HEIGHT (km)
D
N
A
D
N
A
Model AL
Model AH
D - Day
N - Night
A - Average
10^6
10^7
10^8
10^9
ON NUMBER DENSITY (cm^{-3})

Figure 2

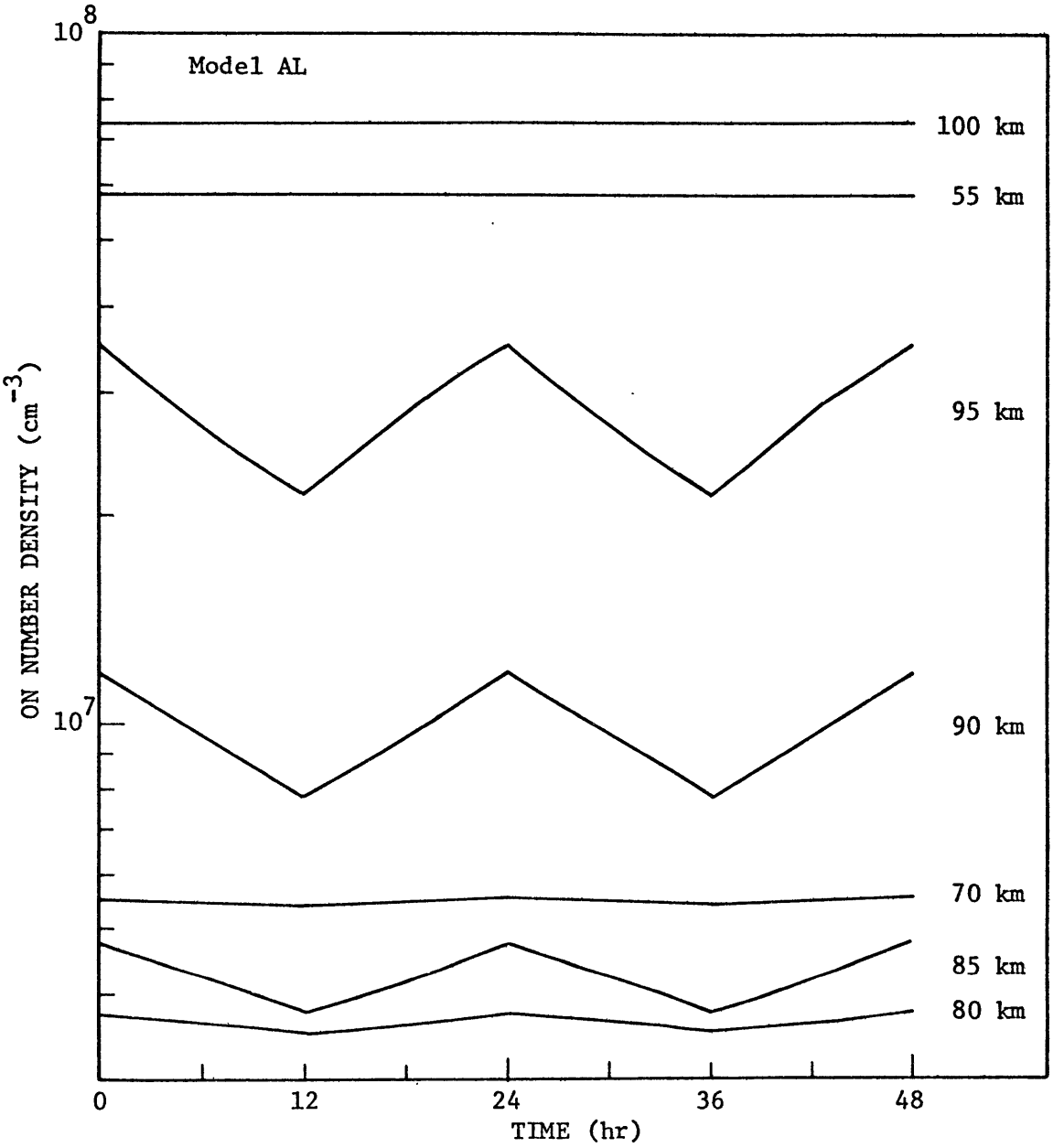
Model AL
10^8
10^7
ON NUMBER DENSITY (cm^{-3})
100 km
55 km
95 km
90 km
70 km
85 km
80 km
0
12
24
36
48
TIME (hr)

Figure 3

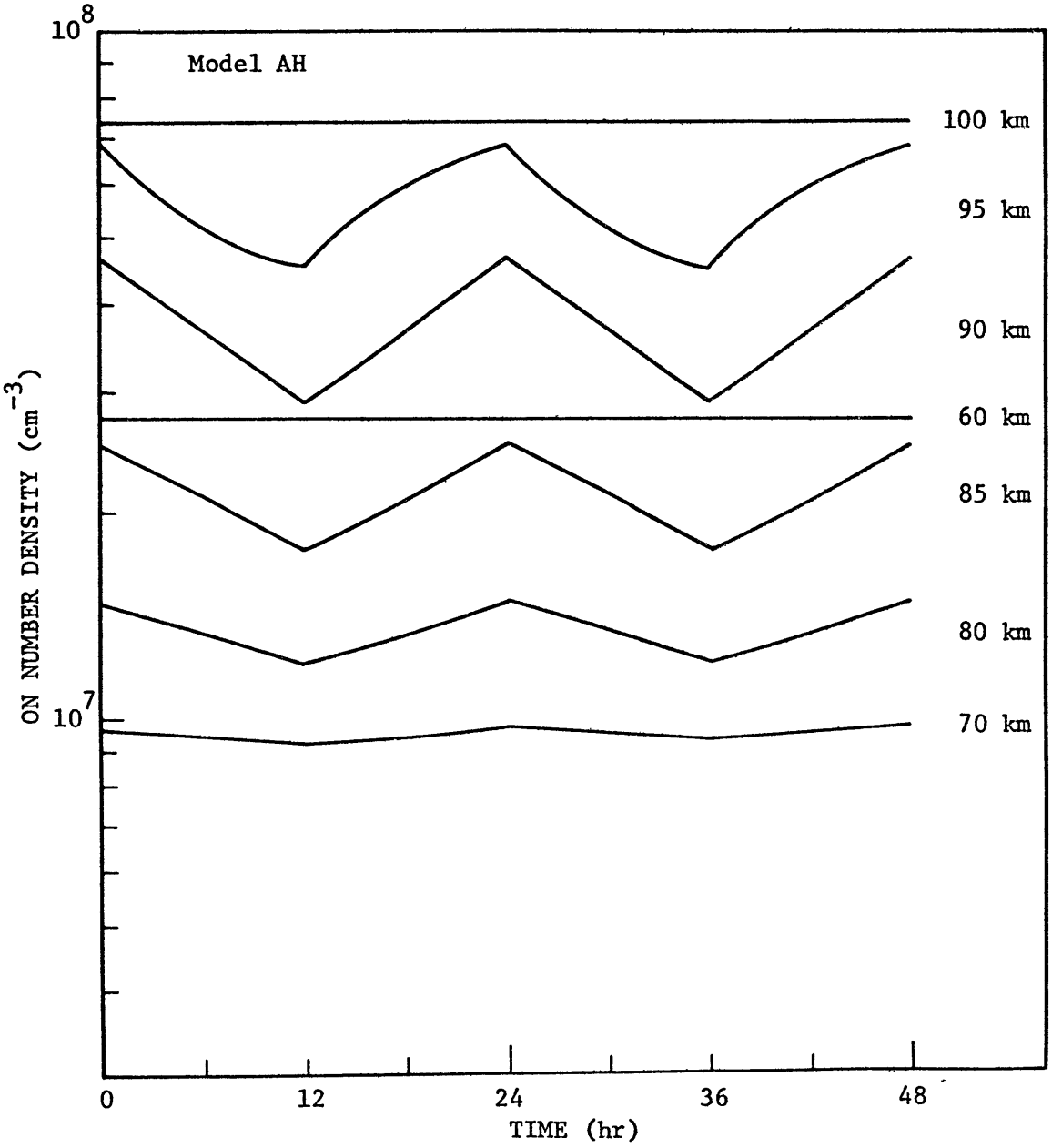
Model AH
10^8
10^7
ON NUMBER DENSITY (cm^{-3})
100 km
95 km
90 km
60 km
85 km
80 km
70 km
0
12
24
36
48
TIME (hr)

Figure 4

increase, respectively, exponentially, except for the model AH concentrations at 95 km which are somewhat asymmetric and non-exponential. Since the concentrations decrease, at the most, by approximately 60 percent, a linear average of the initial and final daytime concentrations will be a very good approximation for the average daytime ON concentration and also for the average nighttime ON concentration because of symmetry. Since the averages will be the same, we can call the value the diurnally averaged ON concentration. The approximation is not as good in the 95 km region of model AH, but it can still be used to give a fairly good diurnally averaged ON concentration.

We can now return to a discussion of the results in Figure 2. As we inferred from time constant considerations, there is no diurnal variation in [ON] in the upper stratosphere and in most of the mesosphere so that a true steady-state has been achieved. In the upper mesosphere and lower thermosphere a diurnal variation was expected and is evident, albeit a small one. Thus, a pseudo steady-state has been attained, as is illustrated in the aforementioned Figures 3 and 4. This pseudo steady-state can be explained by looking at some simple chemical-dynamical arguments. Neglecting eddy transport for a moment, we can describe the ON chemistry in most of the lower thermosphere by the following approximations

$$\frac{d[ON]}{dt} = -2k_2 [N(^4S)][ON] \tag{34}$$

$$[N(^4S)] = J_7 [ON] / k_2 [ON] \tag{35}$$

Combining the two equations, we arrive at the following simple differential equation

$$\frac{d[ON]}{dt} = -2 J_7 [ON] \tag{36}$$

which can be solved for [ON] to yield

$$[ON] = [ON]_o \exp(-2 J_7 t) \tag{37}$$

where $[ON]_o$ is the initial concentration of ON in the daytime. Equation (37) will predict the decay of [ON] during the daytime at some chosen height. For example, for model AH at 90 km, $[ON]_o = 4.65 \times 10^7$ cm^{-3} and $J_7 = 9.60 \times 10^{-6}$ sec^{-1}. For t = 12 hr, the period of our daytime integration, we obtain [ON] = 2.03×10^7 cm^{-3} whereas the actual value is 2.90×10^7 cm^{-3}. For model AL at 90 km, $[ON]_o = 1.18 \times 10^7$ cm^{-3}. For t = 12 hr, we obtain [ON] = 5.15×10^6 cm^{-3} whereas the actual value is 7.76×10^6 cm^{-3}. The odd nitrogen concentration is not allowed to decay to the calculated values because of eddy transport which has a time constant on the order of a day. There is an influx of odd nitrogen from above which replenishes some of the odd nitrogen indirectly lost through photodissociation. At night the chemical production and loss become insignificant and transport dominates (see Tables 3 and 4). The ON is increased, evidently exponentially, by a large flux of ON from above until it attains its initial daytime value. Thus the pseudo steady-state is explained in terms of chemical-dynamical considerations.

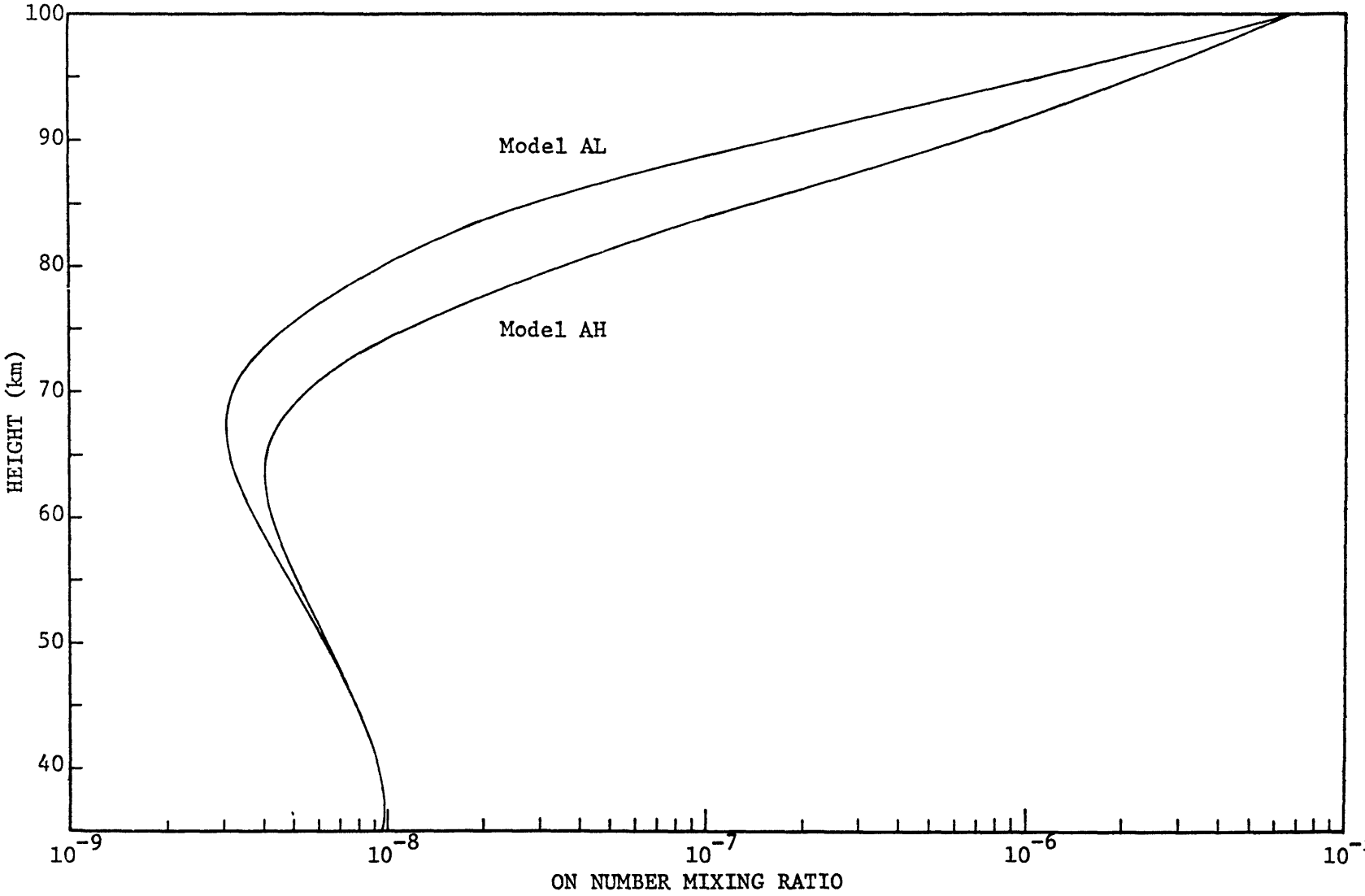
100
90
80
70
60
50
40
HEIGHT (km)
Model AL
Model AH
10^{-9}
10^{-8}
10^{-7}
10^{-6}
10^{-5}
ON NUMBER MIXING RATIO

Figure 5

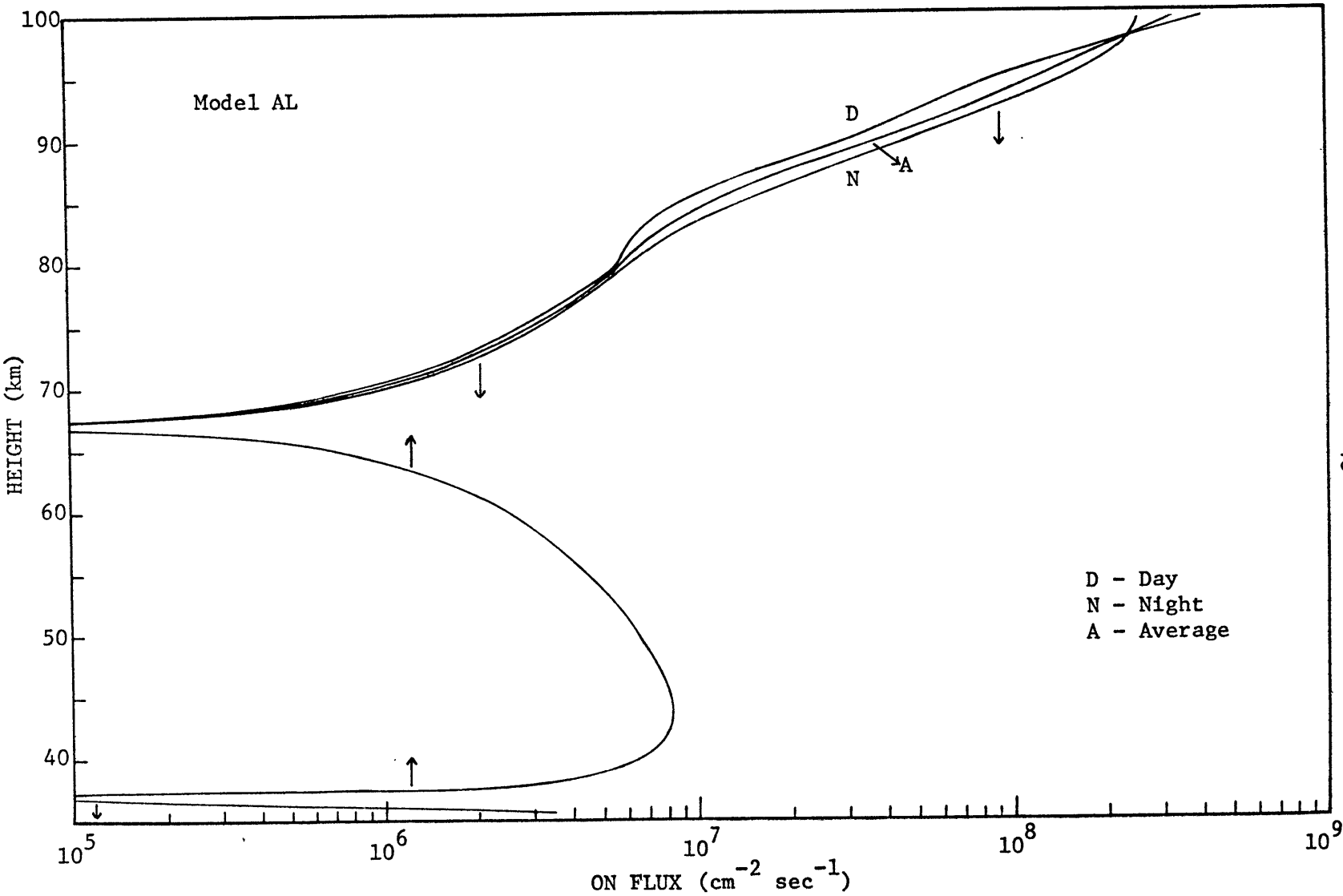
Model AL
D
N
A
D - Day
N - Night
A - Average
HEIGHT (km)
100
90
80
70
60
50
40
10^5
10^6
10^7
10^8
10^9
ON FLUX (cm^{-2} sec^{-1})

Figure 6

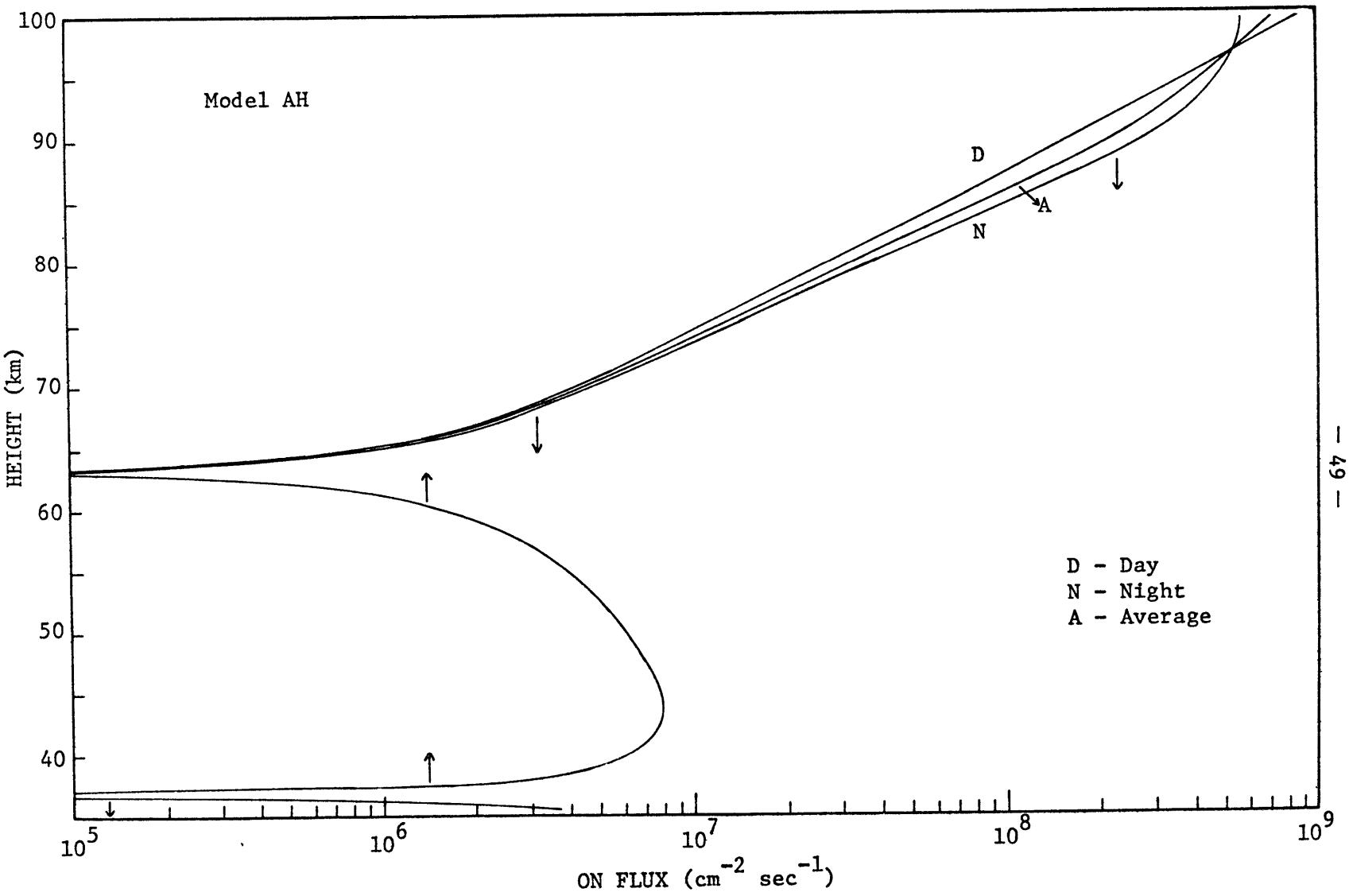
Model AH
D
A
N
D - Day
N - Night
A - Average
HEIGHT (km)
100
90
80
70
60
50
40
10^5
10^6
10^7
10^8
10^9
ON FLUX (cm^{-2} sec^{-1})

Figure 7

After looking at the model results in Figure 2, we can conclude that the choice of the eddy diffusion coefficient profile in the lower thermosphere is very important in determining the equilibrium [ON] profile in the lower thermosphere and upper mesosphere. In other words, transport of odd nitrogen by eddy diffusion is a vital factor in this region and must be examined. In Figure 5 we have depicted the average ON mixing ratio profiles for models AL and AH. We can infer from these profiles that there is a strong downward flux of odd nitrogen in the lower thermosphere, a weaker downward flux in the upper mesosphere, and a small upward flux in most of the upper stratosphere and in the lower mesosphere. Points of zero flux occur between 35 and 40 km and between 60 and 70 km. These inferences are confirmed by the ON fluxes shown in Figures 6 and 7 for models AL and AH. The average fluxes were computed by averaging the fluxes obtained at the end of the daytime and nighttime integrations. In both models the nighttime fluxes are greater than the daytime fluxes except at the very top of the model where the converse is true. It is clear that a strong downward flux of ON exists in the lower thermosphere while a weaker downward flux is present in the upper mesosphere. There is also a small upward flux of odd nitrogen from the upper stratosphere into the lower mesosphere, and a small downward flux at the very bottom of both models. Points of zero flux can be found in both models at approximately 37 km, and at approximately 63 km in model AH and 67 km in model AL. These points exist because there are no strong sources or sinks of ON immediately above or below these levels. Finally, the model AH fluxes are much stronger than the model AL fluxes in the lower thermosphere and upper mesosphere.

The sources of odd nitrogen for these large fluxes into the top of the model are the large production rates of $N(^2D)$ above 100 km via reactions 31, 32, and 34, and predissociation of N_2 in the absorption bands between 800 and 1000 Å. The $N(^2D)$ then reacts with O_2 (reaction 9) to produce NO concentrations of approximately 1×10^8 cm^{-3} in the 100-110 km region (Meira, 1971; Ogawa and Shimazaki, 1975). A calculation of the $N(^2D)$ production rates and the NO production rate from reaction 9 can be found in Strobel et al. (1975) for the region above 100 km. Furthermore, an estimate of the flux into the top of the model can be made by using Meira's (1971) NO observations. With a K of 4.5×10^6 cm^2 sec^{-1}, the NO flux at 100 km is -1.0×10^9 cm^{-2} sec^{-1}; with $K = 1.0 \times 10^6$ cm^2 sec^{-1}, the NO flux at 100 km is -2.9×10^8 cm^{-2} sec^{-1}. The D_{NO} value is 4.0×10^5 cm^2 sec^{-1}. These fluxes are very similar to the fluxes obtained from the model AL and AH calculations.

In order to understand the interaction between chemistry and dynamics in the models and to explain the shape of the profiles in Figure 2, we will refer to the previously mentioned flux convergences and chemical production and loss rates for models AH and AL in Tables 3 and 4, respectively. During the daytime in both models, there is a significant loss of odd nitrogen via reaction 2 throughout almost the entire height range of the model, except at the bottom where there is a small net production of ON via reaction 54. The loss is strongest in the lower thermosphere. The primary source of atomic nitrogen for this loss is photodissociation of nitric oxide, reaction 7. At equilibrium this loss is partly balanced by a flux convergence of odd nitrogen throughout almost the entire height range of the model, except at the bottom where the flux diverges. As we would expect, the convergence is stron-

gest in the lower thermosphere. At night the chemistry changes radically. Reaction 7 no longer operates; the sources of $N(^4S)$ are now dissociation of N_2 by cosmic rays (production rate r_{59}) in the upper stratosphere, mesosphere, and the bottom of the lower thermosphere, and dissociative recombination of NO^+, reaction 32, in the lower thermosphere. Reaction 54 is not a factor. However, these sources are very small and result in very small chemical production and loss rates in the entire height range of the model. Transport now predominates with the flux convergence providing the remainder of the odd nitrogen lost during the daytime. At the bottom of the model the flux diverges in order to balance the remaining odd nitrogen produced during the daytime. Thus, the shape of the individual ON density profiles in Figure 2 is essentially a consequence of nitric oxide being photodissociated to produce $N(^4S)$ which recombines with NO to produce molecular nitrogen; the large daytime and nighttime ON fluxes into the top of the model mitigate this loss somewhat. The difference between the model AL and model AH equilibrium density profiles in the lower thermopshere and upper mesosphere can be explained in terms of the large difference in transport times between the two models. In model AH transport by eddy diffusion is much faster than in model AL, thus not allowing the chemistry to reduce the concentration of ON as much as in model AL by the time equilibrium is reached. In model AL the chemistry is a much larger factor because the transport of ON is not as fast; thus the ON concentration is reduced further by the time equilibrium is attained. Although transport by molecular diffusion is included from 90-100 km, its effect is small when compared to eddy transport.

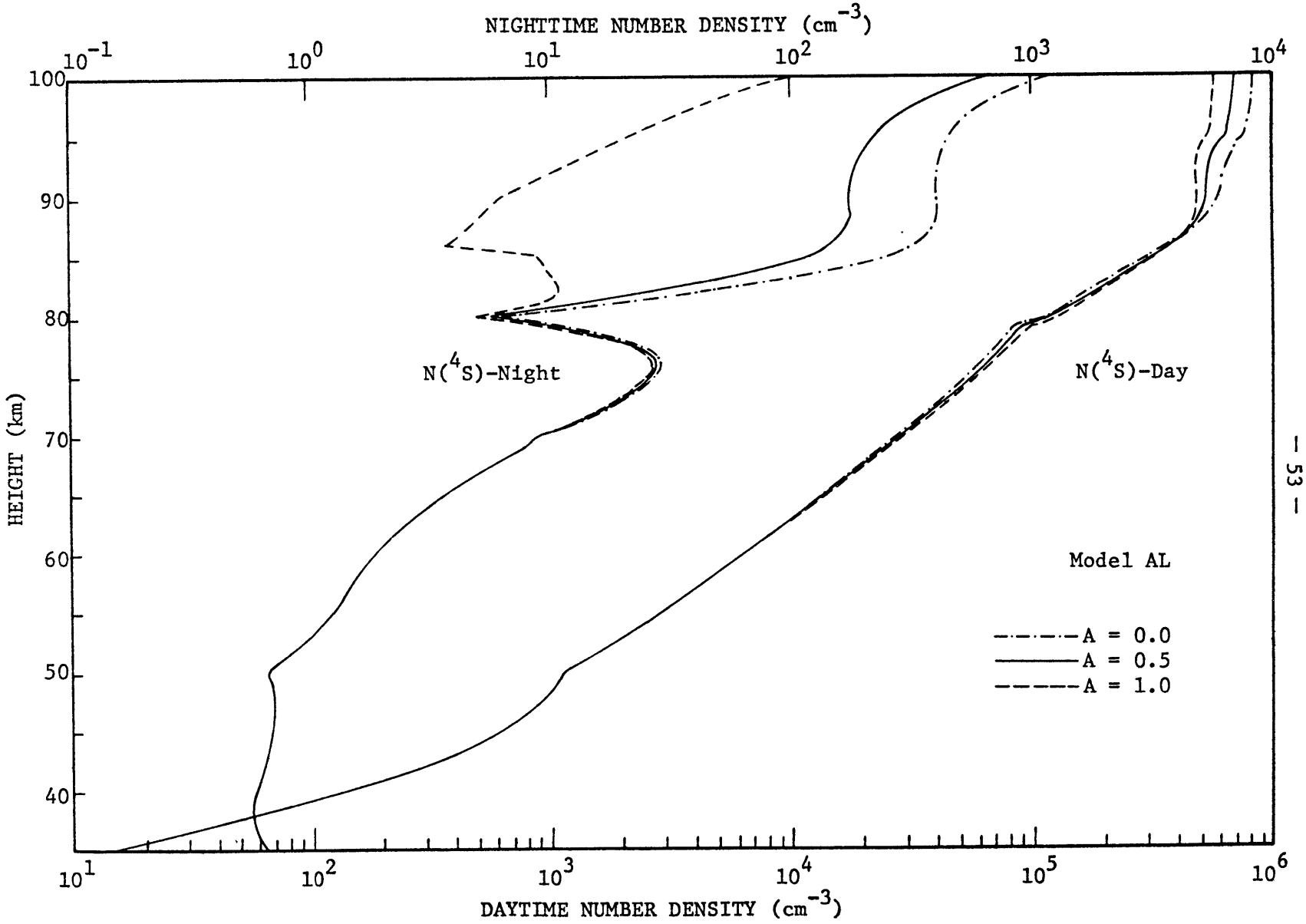
NIGHTTIME NUMBER DENSITY (cm^{-3})
10^{-1}
10^{0}
10^{1}
10^{2}
10^{3}
10^{4}
100
90
80
70
60
50
40
HEIGHT (km)
N(^{4}S)-Night
N(^{4}S)-Day
Model AL
A = 0.0
A = 0.5
A = 1.0
10^{1}
10^{2}
10^{3}
10^{4}
10^{5}
10^{6}
DAYTIME NUMBER DENSITY (cm^{-3})

Figure 8

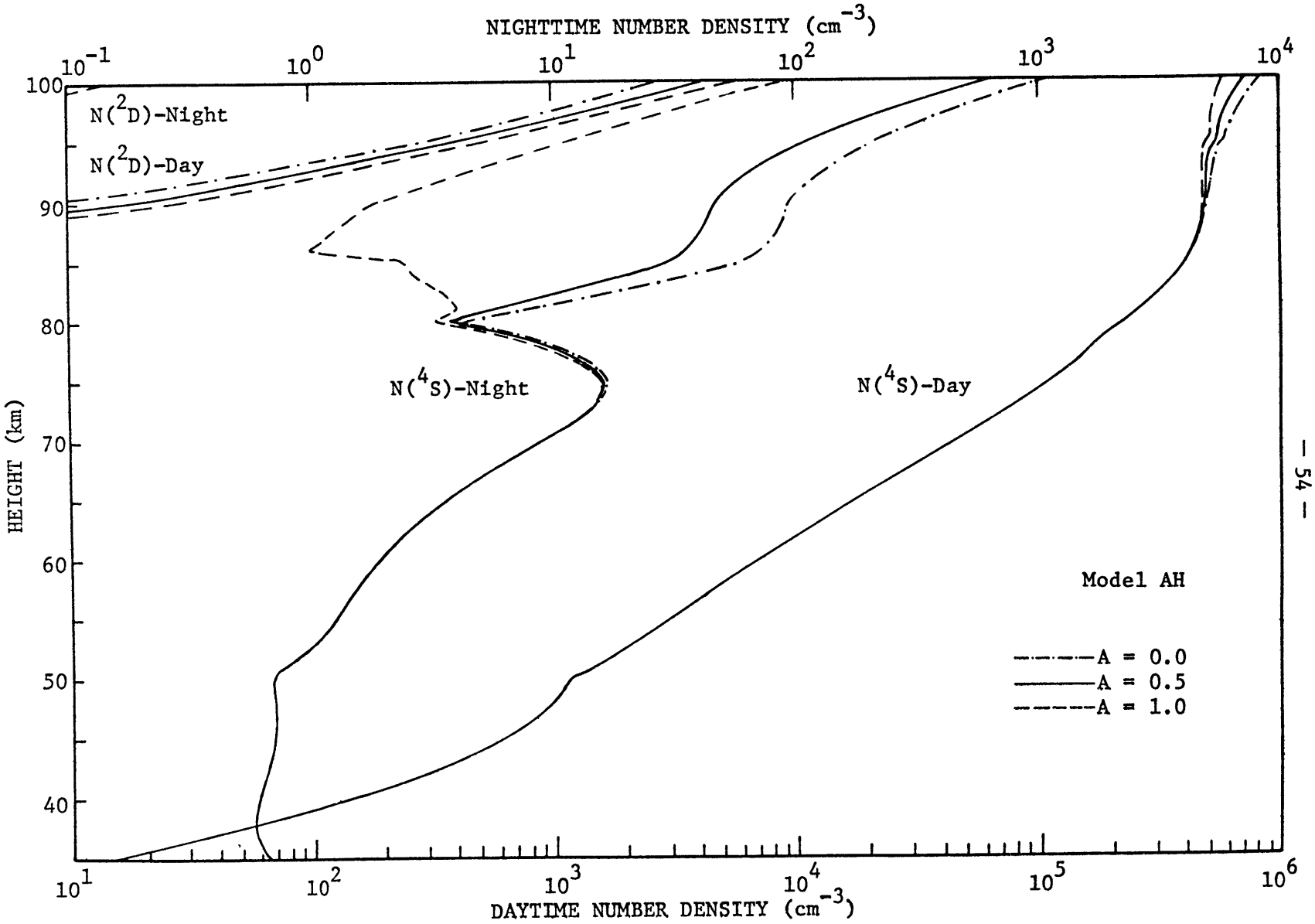
NIGHTTIME NUMBER DENSITY (cm^{-3})
10^{-1}
10^{0}
10^{1}
10^{2}
10^{3}
10^{4}
100
90
80
70
60
50
40
HEIGHT (km)
$N(^2D)$-Night
$N(^2D)$-Day
$N(^4S)$-Night
$N(^4S)$-Day
Model AH
A = 0.0
A = 0.5
A = 1.0
10^{1}
10^{2}
10^{3}
10^{4}
10^{5}
10^{6}
DAYTIME NUMBER DENSITY (cm^{-3})

Figure 9

Since atomic nitrogen in the (^4S) state plays an important role in the chemical loss reaction for odd nitrogen, we have illustrated the daytime and nighttime [$N(^4S)$] profiles for models AL and AH and for various values of parameter A in Figures 8 and 9. Some [$N(^2D)$] profiles, which are the same for both models, are also shown in Figure 9. All of the profiles were calculated by assuming photochemical steady-state. We will now discuss the [$N(^4S)$] profiles from the standpoint of determining which reactions are important in calculating these profiles. We will refer to the expressions for these reactions that can be found in the Model Formulation section. We will also discuss the importance of the reactions which are included in the chemical production and loss expressions for odd nitrogen. We will refer to the model AL profile (with A = 0.5) although the comments will be just as valid for the model AH profile except for those reactions involving [ON] which are even more important in model AH since the equilibrium ON densities are larger in the upper mesosphere and lower thermosphere. The effects of variations in parameter A will be discussed later.

In the daytime upper stratosphere Equations (9) and (10) were used to describe the odd nitrogen chemistry. In Equation (10) for [$N(^4S)$], reaction 7 is an important source of $N(^4S)$ while production rate r_{59} is a very small source and can be neglected. As far as loss processes are concerned, reactions 3 and 5 are important while reactions 2 and 14 can be neglected. In Equation (9), the expression for chem, reaction 54 is very important in the lower part of the upper stratosphere while reaction 2 is very important in the upper part. Production rate r_{59} is relatively unimportant but was included since chem undergoes a sign change in

this region. Reactions 14a, 14b, and 14c are not important and can be neglected. In the daytime mesosphere Equations (12) and (13) describe the ON chemistry. Reaction 2 in Equation (12) is obviously important since it is the primary loss process for ON in the mesosphere. There are no important sources of ON. In Equation (13) for $[N(^4S)]$, reaction 7 is the only important source of $N(^4S)$. As far as loss processes are concerned, reactions 2, 3, and 5 are significant in the entire mesosphere with reaction2 becoming more important in the upper mesosphere along with reaction 16. Reaction 4 can be neglected. In the daytime lower thermosphere Equations (14) and (15) describe the ON chemistry. In Equation (14), the expression for chem, production rate r_{31} and reactions 1 and 34 are small sources of ON while reaction 35 can be omitted. Reaction 2 predominates in this region. In Equation 15 for $[N(^4S)]$, reaction 7 is the most important source of $N(^4S)$ while reactions 1, 20, and 32, and production rate r_{31} are small sources. Reactions 17 and 35 can be neglected. With regard to loss processes, the following reactions vary in their degree of significance depending on the altitude: 3, 5, and 16. Reaction 2 is important throughout the entire region. Reactions 4, 25, and 39 can be omitted.

At night the odd nitrogen chemistry undergoes a significant change, as was discussed previously. We can see in Figures 8 and 9 that the nighttime $N(^4S)$ densities are appreciably less than the daytime densities throughout almost the entire height range of the model. For the height range 35-60 km Equations (22) and (23) describe the ON chemistry. In Equation (22) production rate r_{59} is very important while reactions 14a, 14b, and 14c are relatively unimportant. In Equation (23) for $[N(^4S)]$,

production rate r_{59} is the only important source of $N(^4S)$ while reactions 3 and 5 are significant loss processes. Reaction 14 is a relatively unimportant loss process. For the height range 61-78 km Equations (25) and (26) describe the odd nitrogen chemistry. In Equation (25) r_{59} is still an important source of ON while reaction 2 becomes more significant with increasing altitude. In Equation (26) for $[N(^4S)]$, production rate r_{59} is an important source of $N(^4S)$ while reaction 32 can be neglected. As far as loss processes are concerned, reactions 3 and 5 are significant; reaction 2 becomes more important with increasing altitude, and reaction 16 is important in the upper part of this region. For the height range 79-100 km Equations (27) and (28) describe the odd nitrogen chemistry. In Equation (27) the production rate r_{59} disappears by 85 km while reaction 2 is very important throughout the entire height range. In Equation (28) for $[N(^4S)]$, reaction 32 is a very important source of $N(^4S)$ while reactions 17 and 20 are relatively unimportant unless A = 1.0. Production rate r_{59} disappears by 85 km. With regard to loss processes, reaction 16 is only important up to approximately 85km; reactions 3 and 5 are relatively unimportant. Reaction 2 is very important while reaction 25 can be neglected. A brief comment should be made about the dip in $[N(^4S)]$ around 80 km. This dip is the result of an increase and then a decrease in the nighttime OH concentrations around 80 km.

We can now discuss the effects of variations in parameter A on the odd nitrogen and atomic nitrogen density profiles. Figure 10 depicts the average equilibrium odd nitrogen density profiles obtained by varying A from 0.0 to 1.0 in models AL and AH. If A = 0.0 in reaction 32, all the atomic nitrogen produced is in the (^4S) ground state; if A = 1.0,

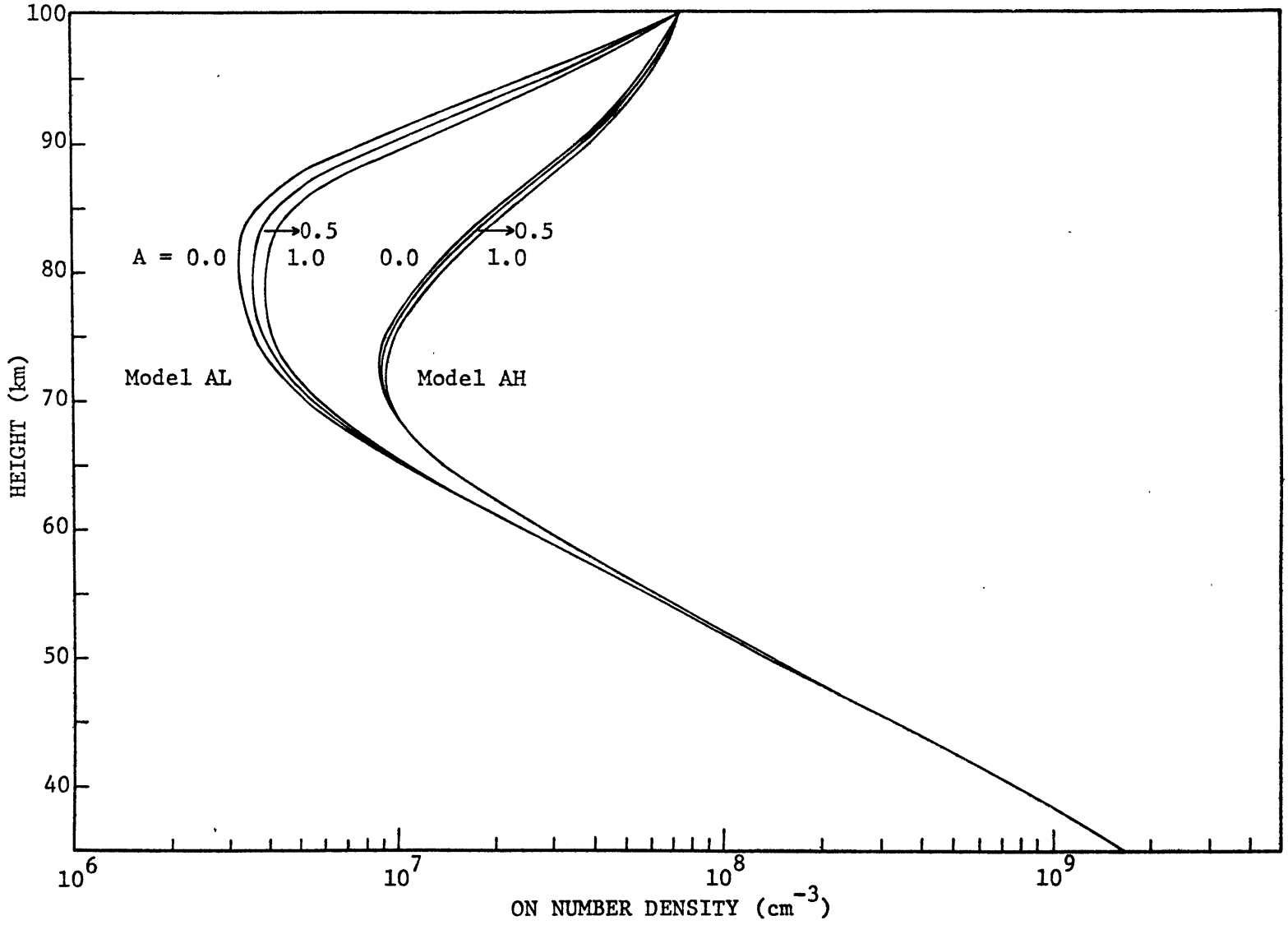
100
90
80
70
60
50
40
HEIGHT (km)
A = 0.0
0.5
1.0
0.0
0.5
1.0
Model AL
Model AH
10^6
10^7
10^8
10^9
ON NUMBER DENSITY (cm^{-3})

Figure 10

all the atomic nitrogen is in the (^2D) excited state. For model AH changes in A do not alter appreciably the average [ON] profiles. The effect upon the atomic nitrogen density profiles can be seen in Figure 9. The daytime [$N(^4S)$] profile is affected slightly from approximately 90-100 km. This small change, however, does affect, albeit slightly, the ON density profiles all the way down to the upper mesosphere. The reason for the small change in daytime [$N(^4S)$] is that reaction 32 only provides a small source of $N(^4S)$ while reaction 7 is the major source, especially in model AH since the ON concentrations are much higher than those in model AL in the lower thermosphere. Nighttime [$N(^4S)$] shows a very large change since reaction 32 is the major source of $N(^4S)$. If A = 0.0, [$N(^4S)$] is maximum; if A = 1.0,[$N(^4S)$] is minimum. The same behavior is evident during the daytime. However, the nighttime chemistry does not affect the [ON] profiles since transport is the predominating factor at night. For model AL changes in A result in significantly larger changes in the [ON] profiles. The effect upon [$N(^4S)$] can be seen in Figure 8. Greater changes are evident in the daytime [$N(^4S)$], and these result in changes in the [ON] profiles all the way down to the upper mesosphere. In the upper part of the lower thermosphere, if A = 0.0, [$N(^4S)$] is maximum; if A = 1.0, [$N(^4S)$] is minimum. The same is true during the nighttime. However, the opposite occurs for daytime [$N(^4S)$] in the lower part of the lower thermosphere and in the upper mesosphere although the change is very small. This behavior is the result of the ON density change affecting reactions 2 and 7 in the expression for [$N(^4S)$]. The reason for the larger change in the [ON] profiles in model AL is that chemistry is a more important factor than in model AH because eddy transport is not as fast. In both models if A = 0.0, more $N(^4S)$ is available at any particular moment for recombination with NO thus decreasing the ON concentration.

Since reaction 32 has its largest impact in the upper part of the lower thermosphere, smaller ON concentrations probably decrease the amount of ON available for transport into the rest of the lower thermosphere and upper mesosphere, thereby decreasing the ON concentrations in those regions. If A = 1.0, the opposite occurs. These effects can be seen in Figure 10. In this study we decided to use A = 0.5 as a representative value for parameter A since the correct ratio of $N(^4S)$ to $N(^2D)$ production is not known. It is also evident from this discussion that large changes in A will not affect the results greatly.

Having presented the important results of models AL and AH, we can now briefly compare these results with actual measurements. In Figure 11 we have illustrated the average equilibrium odd nitrogen density profiles for models AL and AH along with nitric oxide denisty profiles calculated from rocket measurements of the dayglow NO emission rate in the $\gamma(1,0)$ band by Meira (1971) and by Barth (1966). In the region of comparison above approximately 70 km, the average odd nitrogen density profiles are equivalent to average nitric oxide density profiles since odd nitrogen is almost entirely in the form of nitric oxide in this region during both the daytime and nighttime. It is obvious that the comparison is not very good except for the model AH profile above approximately 80 km. However, it is mentioned in Strobel (1972b) that Meira's data are not really sensitive to mesospheric NO because the major contribution to the $\gamma(1,0)$ band emission comes from NO above 95 km. Also, Meira's results are not easily reconciled with current models of D-region chemistry since they lead to electron densities approximately a factor of 10 larger than observed electron densities. In our model we have used observed daytime

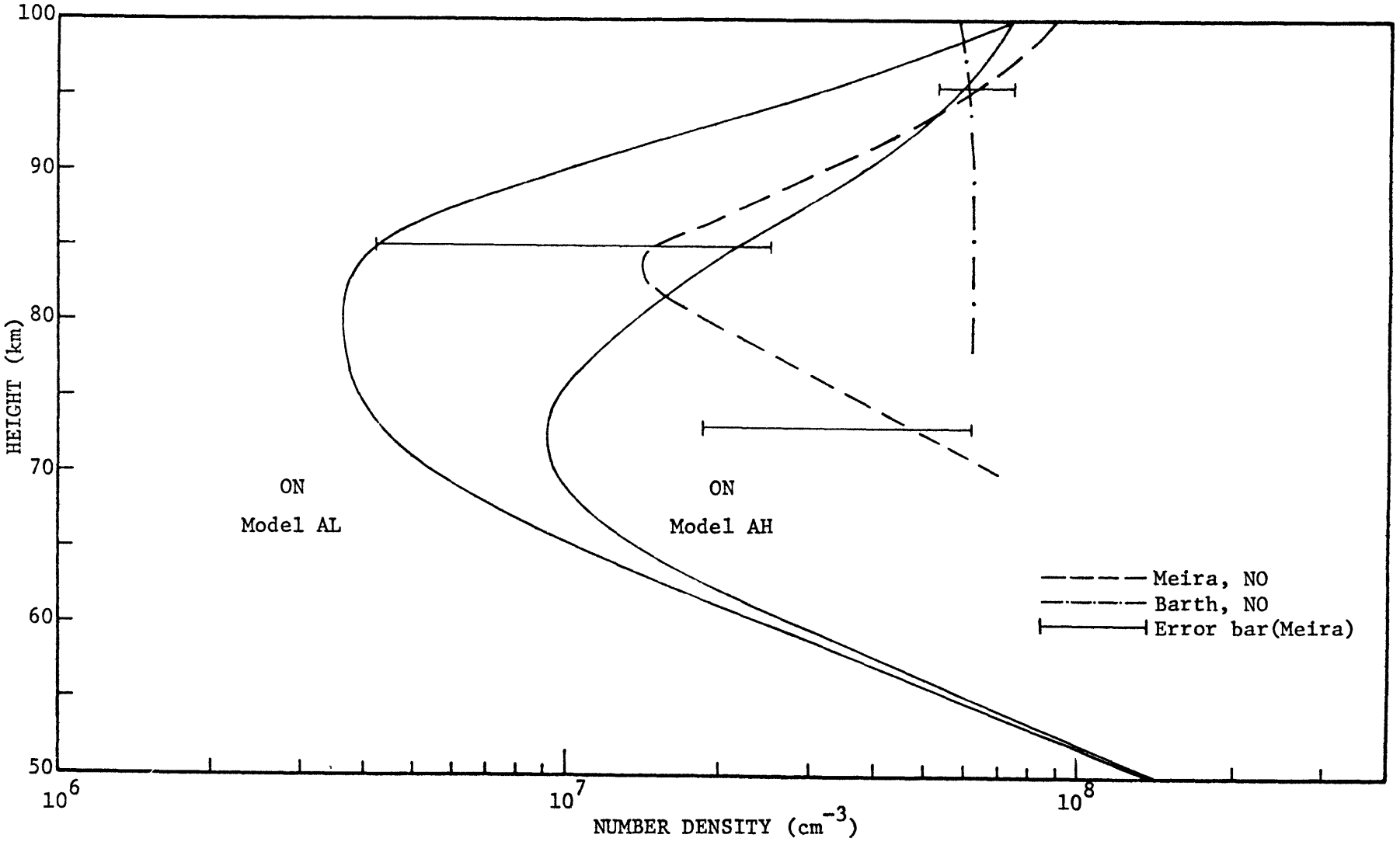
100
90
80
70
60
50
HEIGHT (km)
ON
Model AL
ON
Model AH
Meira, NO
Barth, NO
Error bar(Meira)
10^6
10^7
10^8
NUMBER DENSITY (cm^{-3})

Figure 11

electron densities. This is recommended by Strobel (1972b) who argues for reduced NO concentrations in the mesosphere similar to those obtained in our model AL. Our results are in good agreement with the results obtained by Strobel (1972b) and by Ogawa and Shimazaki (1975).

At this point a few comments can be made about the assumption that the boundary conditions would not vary diurnally. At the lower boundary this is a valid assumption since no diurnal variation in odd nitrogen is observed in the upper stratosphere because of the long chemical and dynamical time constants. At the upper boundary the assumption is probably not as good because of the small diurnal variation obtained in the lower thermosphere. However, nighttime observations of NO were not available. We will assume that this approximation is reasonably good since the diurnal variations in the lower thermosphere are relatively small.

The model was also run with a smaller K profile in the upper stratosphere and mesosphere in order to see what effect this profile would have on the ON concentration profile. Two variations of this smaller K profile were investigated: model BL and model BH (see Input Data section for discussion of profiles). The results can be seen in Figures 12 and 13 which compare the average equilibrium odd nitrogen density profiles obtained from the previous models with the density profiles obtained by using the lower K profile. The old and new K profiles are equivalent in the lower thermosphere. In Figure 12 the results of models AL and BL are compared. The model BL [ON] profile is slightly higher in the lower part of the upper stratosphere and is somewhat lower in the upper part of the stratosphere and in the mesosphere than the model AL [ON] profile.

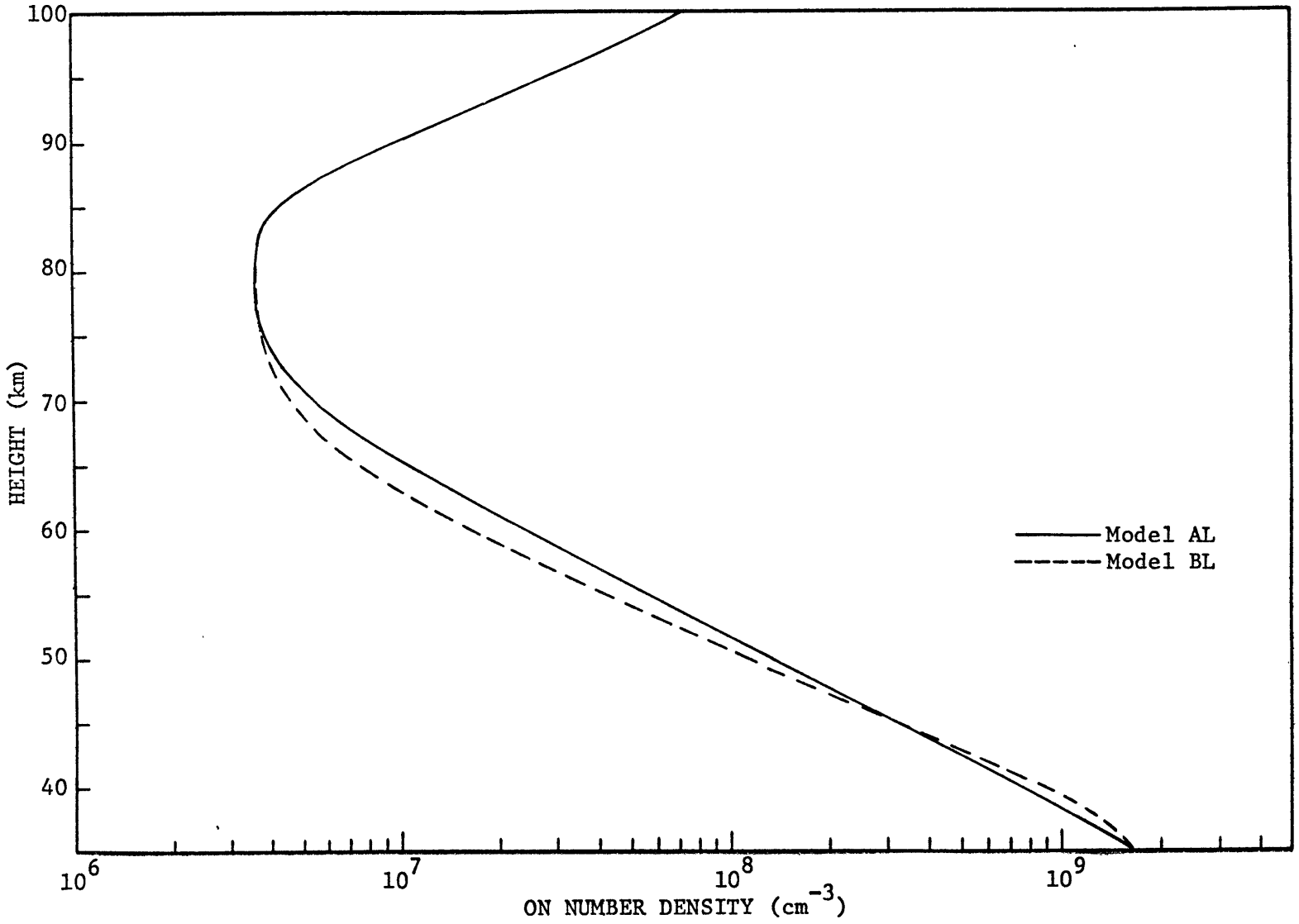
100
90
80
70
60
50
40
HEIGHT (km)
10^6
10^7
10^8
10^9
ON NUMBER DENSITY (cm^{-3})
Model AL
Model BL

Figure 12

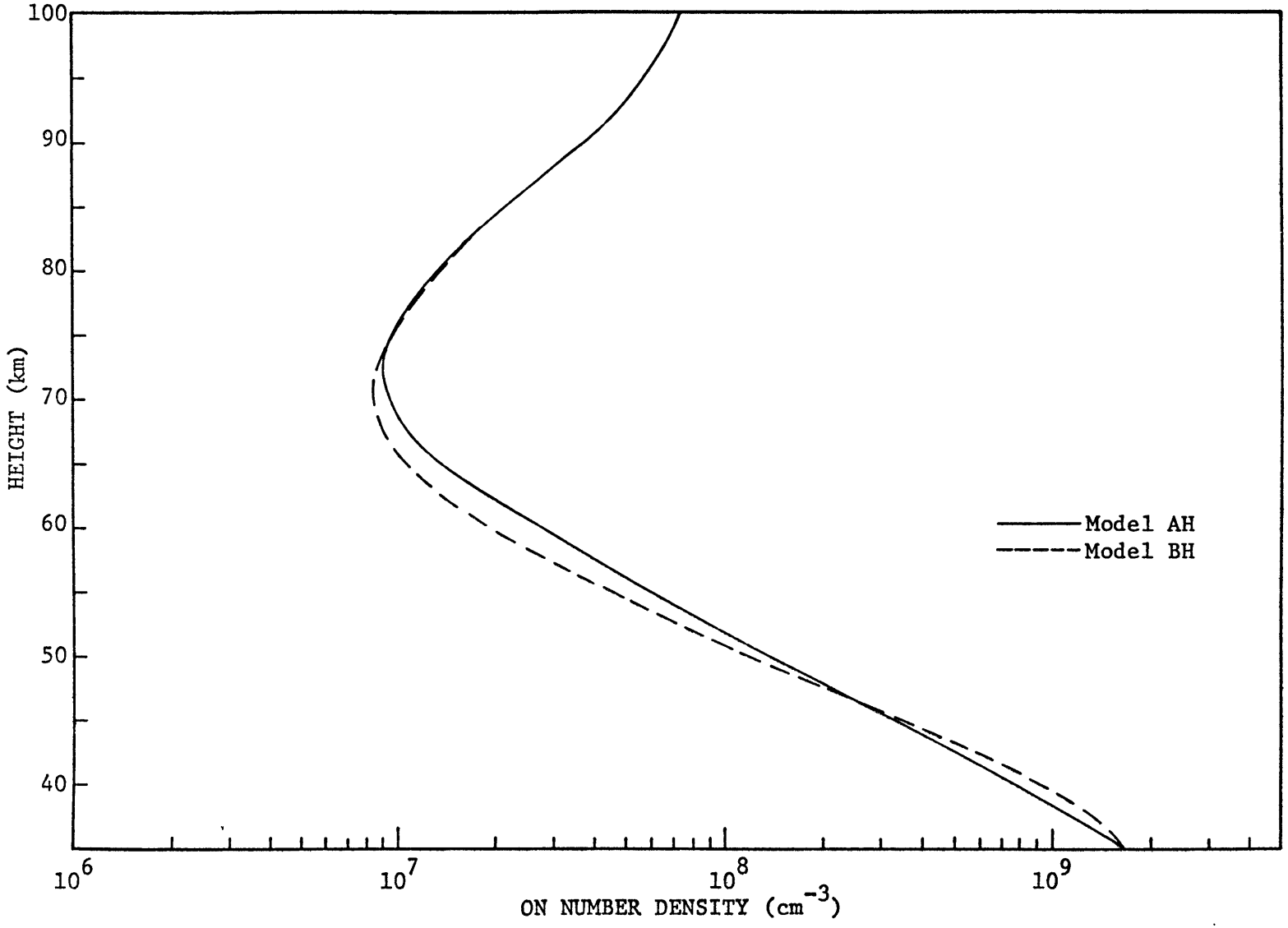
100
90
80
70
60
50
40
HEIGHT (km)
10^6
10^7
10^8
10^9
ON NUMBER DENSITY (cm^{-3})
Model AH
Model BH

Figure 13

The same is true for the model BH [ON] profile versus the model AH [ON] profile in Figure 13. It would appear that lower K values in the upper stratosphere and in the mesosphere do not alter substantially the equilibrium average odd nitrogen density profiles. Chemistry appears to be a greater factor in models BL and BH than in models AL and AH since transport by eddy diffusion is not as fast. Consequently, where changes between the profiles are evident, the chemical loss process reduces the equilibrium ON concentrations in the upper part of the profile, and the chemical production process increases the equilibrium ON concentrations in the lower part of the profile. In the lower thermosphere there is no difference between the old and new [ON] profiles. One can therefore conclude that changes in mesospheric and upper stratospheric K values will probably have no effect on [ON] profiles in the lower thermosphere.

We have also compared the average vertical fluxes of odd nitrogen for models AH and BH in Figure 14. It is evident that the fluxes are similar in magnitude and direction. The fluxes in model BH in the upper stratosphere and in the mesosphere are somewhat lower than the fluxes in model AH. A comparison of the model BL and AL average fluxes will give similar results. Finally, the points of zero flux for model BL occur at approximately 38 and 65 km; for model BH at approximately 38 and 62 km.

We will conclude this section by depicting in Figure 15 a number of different odd nitrogen species during the daytime and nighttime for models AH and BH. Most of the relevant chemistry for this illustration was discussed in the Model Formulation section. Many of the profiles were calculated by assuming photochemical steady-state. The daytime and

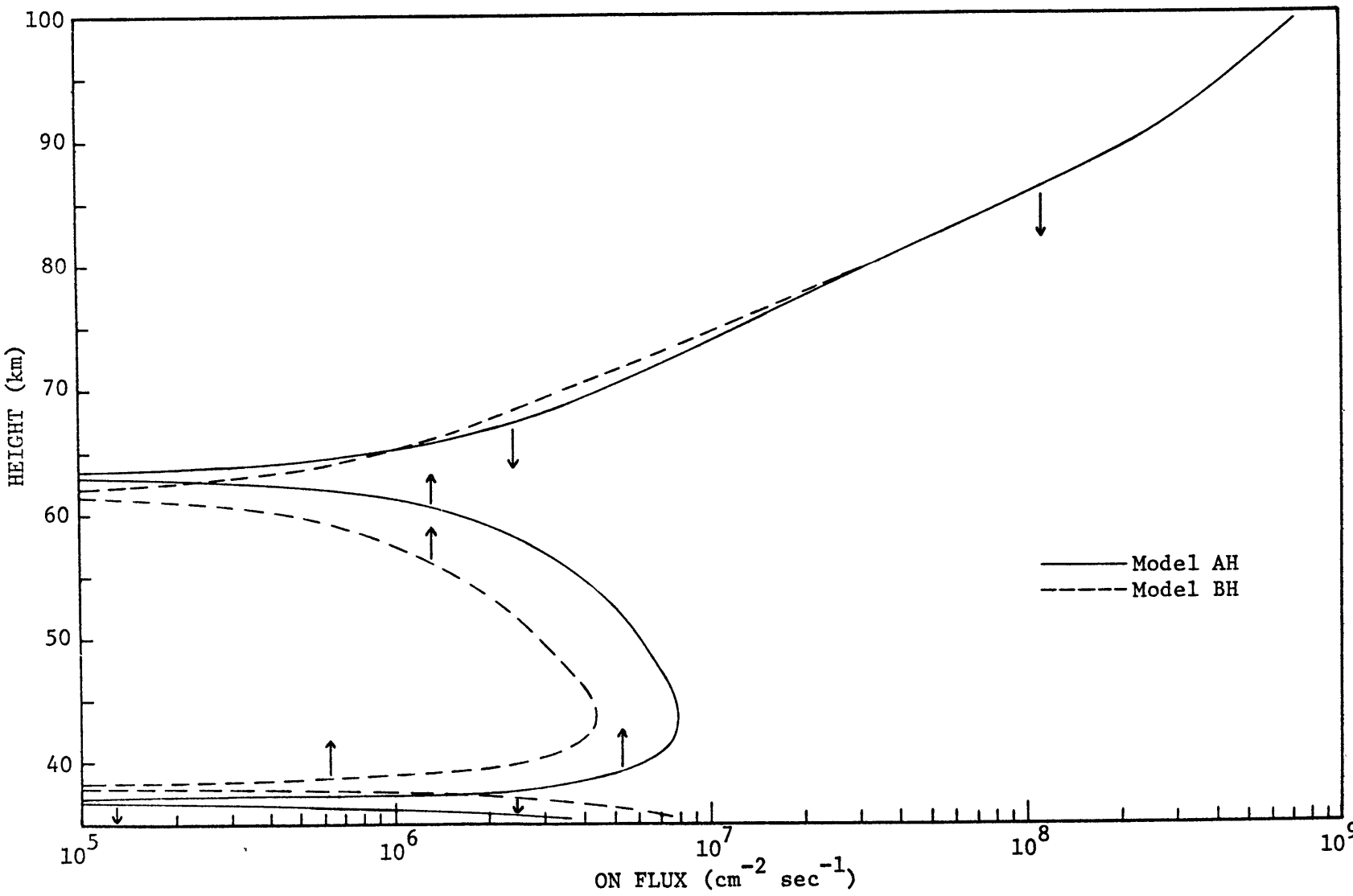
100
90
80
70
60
50
40
HEIGHT (km)
Model AH
Model BH
10^5
10^6
10^7
10^8
10^9
ON FLUX (cm^{-2} sec^{-1})

Figure 14

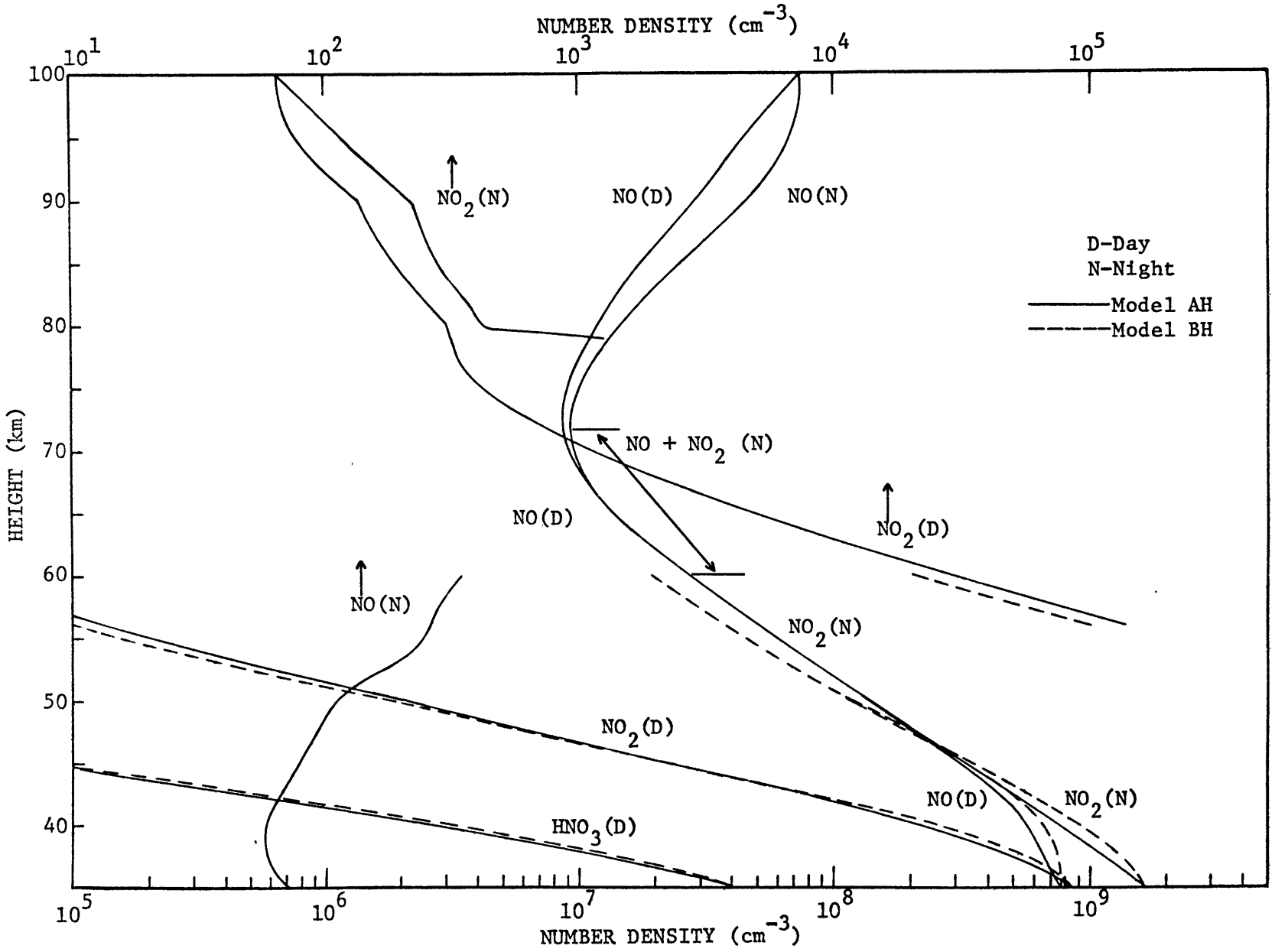
NUMBER DENSITY (cm^{-3})
10^1
10^2
10^3
10^4
10^5
100
90
80
70
60
50
40
HEIGHT (km)
NO_2(N)
NO(D)
NO(N)
D-Day
N-Night
Model AH
Model BH
NO + NO_2 (N)
NO(D)
NO_2(D)
NO(N)
NO_2(N)
NO_2(D)
NO(D)
NO_2(N)
HNO_3(D)
10^5
10^6
10^7
10^8
10^9
NUMBER DENSITY (cm^{-3})

Figure 15

nighttime profiles were determined by using values at the end of the daytime and nighttime integrations. This point is relevant in the upper mesosphere and the lower thermosphere where a diurnal variation exists. It is evident that there is very little difference between the density profiles obtained in the upper stratosphere and lower mesosphere with the model AH and BH K profiles, as would be expected from the previous discussion. It should be noted that the daytime NO_2 density at 35 km is approximately equal to the daytime NO density at 35 km but falls off very rapidly until it is only a small fraction of the daytime NO density at the stratopause.

6. Summary

We have demonstrated a new method for solving a one-dimensional chemical-dynamical model for odd nitrogen. The application of the Lorenz N-cycle scheme coupled with the use of average daytime and nighttime input data results in a steady-state solution in the upper stratosphere and lower mesosphere and a pseudo steady-state solution in the upper mesosphere and lower thermosphere. The odd nitrogen density profiles obtained from this model should be more physically realistic than those from a model which utilizes diurnally averaged data. This method could be applied to other chemical-dynamical systems to simulate their processes as realistically as possible without having to solve a completely time-dependent system.

We should also mention some of the more important chemical and dynamical results. The choice of the eddy diffusion coefficient profile in the lower thermosphere is very important in determining the equilibrium [ON] profile in the lower thermosphere and upper mesosphere. However, changing the K profile in the lower thermosphere appears to have no effect on [ON] in the upper stratosphere and a very small effect on [ON] in the lower mesosphere. Changing mesospheric and upper stratospheric K values appears to have a small effect on [ON] in those regions and no effect on [ON] in the lower thermosphere. There exists a strong downward flux of odd nitrogen into the top of the model and in the lower thermosphere; at the stratopause there is a small upward flux of odd nitrogen. As far as chemistry is concerned, changing the fraction of $N(^4S)$ produced from the dissociative recombination of NO^+ does not

affect the equilibrium [ON] profiles greatly; a slightly larger effect is noticeable when a smaller K profile is used in the lower thermosphere.

APPENDIX A

Profiles of Input Data

All of the input concentration profiles (units cm^{-3}) along with profiles for production rates r_{31} and r_{59} (units cm^{-3} sec^{-1}), photodissociation rates J_1, J_7, and J_{58} (units sec^{-1}), and temperature T (units °K) are included in this appendix. The notation used to represent powers of ten is the following: value±x = value x $10^{\pm x}$. Nighttime concentrations are identified by the subscript "n".

z(km)	T	$[N_2]$	$[O_2]$	[O]	[M]	[OH]
35	240.3	.1380+18	.3700+17	.2400+9	.1750+18	.4000+7
36	242.3	.1189+18	.3187+17	.3429+9	.1508+18	.4060+7
37	244.4	.1027+18	.2749+17	.4817+9	.1301+18	.4120+7
38	246.4	.8871+17	.2375+17	.6650+9	.1125+18	.4180+7
39	248.5	.7675+17	.2055+17	.9017+9	.9730+17	.4240+7
40	250.5	.6650+17	.1780+17	.1200+10	.8430+17	.4300+7
41	252.6	.5769+17	.1544+17	.1566+10	.7313+17	.4360+7
42	254.6	.5011+17	.1341+17	.2004+10	.6352+17	.4420+7
43	256.7	.4068+17	.1090+17	.2512+10	.5528+17	.4480+7
44	258.7	.3797+17	.1017+17	.3082+10	.4814+17	.4540+7
45	260.8	.3310+17	.8870+16	.3700+10	.4197+17	.4600+7
46	262.8	.2888+17	.7739+16	.4297+10	.3662+17	.4560+7
47	264.9	.2522+17	.6759+16	.4888+10	.3198+17	.4520+7
48	266.9	.2196+17	.5885+16	.5461+10	.2784+17	.4480+7
49	269.0	.1923+17	.5155+16	.6000+10	.2439+17	.4440+7
50	271.0	.1690+17	.4530+16	.6500+10	.2143+17	.4400+7
51	268.2	.1499+17	.4018+16	.7012+10	.1901+17	.4590+7
52	265.5	.1333+17	.3574+16	.7472+10	.1690+17	.4767+7
53	262.7	.1187+17	.3184+16	.7865+10	.1506+17	.4929+7
54	259.9	.1058+17	.2839+16	.8178+10	.1342+17	.5074+7
55	257.2	.9430+16	.2530+16	.8400+10	.1196+17	.5200+7
56	254.4	.8360+16	.2243+16	.7984+10	.1060+17	.5306+7
57	251.6	.7402+16	.1987+16	.7586+10	.9389+16	.5389+7
58	248.8	.6548+16	.1758+16	.7207+10	.8306+16	.5450+7
59	246.1	.5783+16	.1553+16	.6845+10	.7336+16	.5487+7
60	243.3	.5100+16	.1370+16	.6500+10	.6470+16	.5500+7
61	240.6	.4490+16	.1206+16	.6171+10	.5697+16	.5219+7
62	238.0	.3948+16	.1060+16	.5856+10	.5008+16	.4960+7
63	235.3	.3466+16	.9307+15	.5557+10	.4396+16	.4722+7
64	232.6	.3038+16	.8158+15	.5272+10	.3854+16	.4502+7
65	230.0	.2260+16	.7140+15	.5000+10	.3374+16	.4300+7
66	227.3	.2326+16	.6240+15	.4767+10	.2950+16	.4113+7
67	224.6	.2030+16	.5447+15	.4552+10	.2575+16	.3941+7
68	221.9	.1771+16	.4747+15	.4353+10	.2246+16	.3782+7

z(km)	T	$[N_2]$	$[O_2]$	[O]	[M]	[OH]
69	219.3	.1542+16	.4131+15	.4169+10	.1955+16	.3635+7
70	216.6	.1340+16	.3590+15	.4000+10	.1699+16	.3500+7
71	213.5	.1162+16	.3115+15	.3960+10	.1474+16	.3560+7
72	210.5	.1007+16	.2702+15	.3920+10	.1277+16	.3620+7
73	207.4	.8708+15	.2338+15	.3880+10	.1105+16	.3680+7
74	204.4	.7514+15	.2019+15	.3840+10	.9533+15	.3740+7
75	201.3	.6470+15	.1740+15	.3800+10	.8210+15	.3800+7
76	198.2	.5557+15	.1495+15	.5720+10	.7052+15	.3602+7
77	195.2	.4778+15	.1285+15	.7857+10	.6063+15	.3401+7
78	192.1	.4089+15	.1099+15	.1002+11	.5187+15	.3199+7
79	189.1	.3486+15	.9365+14	.1208+11	.4422+15	.2999+7
80	186.0	.2960+15	.7950+14	.1400+11	.3755+15	.2800+7
81	186.0	.2488+15	.6683+14	.1588+11	.3156+15	.2402+7
82	186.0	.2084+15	.5598+14	.1793+11	.2644+15	.1885+7
83	186.0	.1741+15	.4677+14	.2052+11	.2209+15	.1360+7
84	185.9	.1452+15	.3900+14	.2422+11	.1842+15	.9063+6
85	185.9	.1210+15	.3250+14	.3000+11	.1535+15	.5600+6
86	185.9	.1012+15	.2718+14	.4255+11	.1284+15	.3223+6
87	185.9	.8469+14	.2273+14	.6444+11	.1074+15	.1736+6
88	185.9	.7087+14	.1901+14	.1042+12	.8988+14	.8783+5
89	185.8	.5931+14	.1590+14	.1800+12	.7521+14	.4195+5
90	185.8	.4965+14	.1330+14	.3320+12	.6328+14	.1900+5
91	188.4	.4133+14	.1106+14	.4530+12	.5284+14	.8341+4
92	190.9	.3413+14	.9165+13	.5650+12	.4386+14	.3487+4
93	193.5	.2829+14	.7591+13	.6533+12	.3653+14	.1388+4
94	195.9	.2347+14	.6279+13	.7100+12	.3045+14	.2563+3
95	198.2	.1950+14	.5190+13	.7370+12	.2543+14	.1900+3
96	200.4	.1630+14	.4290+13	.7360+12	.2133+14	—
97	202.4	.1367+14	.3544+13	.7095+12	.1792+14	—
98	204.4	.1149+14	.2926+13	.6640+12	.1508+14	—
99	206.3	.9681+13	.2414+13	.6072+12	.1270+14	—
100	208.1	.8180+13	.1990+13	.5480+12	.1072+14	—

z(km)	$[N_2^+]$	$[O^+]$
90	.5400-1	—
91	.7645-1	—
92	.1087+0	—
93	.1551+0	—
94	.2224+0	—
95	.3200+0	.1000+0
96	.4624+0	.2431+0
97	.6709+0	.5480+0
98	.9774+0	.1146+1
99	.1430+1	.2223+1
100	.2100+1	.4000+1

z(km)	$[O_3]$	$[O_3]_n$	$[O_2(^1\Delta_g)]$	J_7	r_{59}
35	.2000+13	.2000+13	—	.2530-7	.9000+0
36	.1878+13	.1865+13	—	.4127-7	.7758+0
37	.1683+13	.1669+13	—	.6436-7	.6706+0
38	.1453+13	.1444+13	—	.9638-7	.5811+0
39	.1215+13	.1215+13	—	.1391-6	.5050+0
40	.1000+13	.1000+13	—	.1940-6	.4400+0
41	.8097+12	.8097+12	—	.2625-6	.3844+0
42	.6477+12	.6477+12	—	.3454-6	.3380+0
43	.4569+12	.5140+12	—	.4434-6	.2971+0
44	.4059+12	.4059+12	—	.5566-6	.2613+0
45	.3200+12	.3200+12	—	.6850-6	.2300+0
46	.2541+12	.2541+12	—	.8297-6	.2020+0
47	.2015+12	.2015+12	—	.9865-6	.1773+0
48	.1592+12	.1592+12	—	.1158-5	.1557+0
49	.1261+12	.1261+12	—	.1345-5	.1367+0
50	.1000+12	.1000+12	.8800+10	.1540-5	.1200+0
51	.7947+11	.7947+11	.1001+11	.1752-5	.1064+0
52	.6321+11	.6321+11	.1127+11	.1974-5	.9578-1
53	.5048+11	.4783+11	.1253+11	.2207-5	.8669-1
54	.4020+11	.3874+11	.1379+11	.2449-5	.7644-1
55	.3200+11	.3200+11	.1500+11	.2700-5	.6800-1
56	.2541+11	.2707+11	.1500+11	.2964-5	.5801-1
57	.2015+11	.2318+11	.1500+11	.3237-5	.4883-1
58	.1592+11	.2000+11	.1500+11	.3518-5	.4290-1
59	.1261+11	.1733+11	.1500+11	.3809-5	.3814-1
60	.1000+11	.1500+11	.1500+11	.4110-5	.3400-1
61	.7947+10	.1302+11	.1376+11	.4431-5	.3092-1
62	.6321+10	.1115+11	.1262+11	.4788-5	.2820-1
63	.5048+10	.9338+10	.1156+11	.5135-5	.2568-1
64	.4020+10	.7610+10	.1059+11	.5479-5	.2330-1
65	.3200+10	.6000+10	.9700+10	.5810-5	.2100-1
66	.2541+10	.4496+10	.8878+10	.6072-5	.1866-1
67	.2015+10	.3253+10	.8121+10	.6311-5	.1648-1
68	.1592+10	.2273+10	.7426+10	.6530-5	.1447-1
69	.1261+10	.1534+10	.6787+10	.6734-5	.1265-1
70	.1000+10	.1000+10	.6200+10	.6930-5	.1100-1
71	.7947+9	.6055+9	.5388+10	.7158-5	.9536-2
72	.6321+9	.3577+9	.4650+10	.7387-5	.8236-2
73	.4941+9	.2081+9	.4004+10	.7634-5	.7088-2
74	.3956+9	.1204+9	.3455+10	.7857-5	.6080-2
75	.3200+9	.7000+8	.3000+10	.8070-5	.5200-2
76	.2645+9	.4292+8	.2680+10	.8258-5	.4441-2
77	.2214+9	.2670+8	.2420+10	.8411-5	.3781-2
78	.1877+9	.1685+8	.2208+10	.8561-5	.3211-2
79	.1611+9	.1078+8	.2037+10	.8700-5	.2721-2
80	.1400+9	.7000+7	.1900+10	.8830-5	.2300-2
81	.1201+9	.1650+8	.2039+10	.8963-5	.1940-2
82	.1030+9	.3141+8	.2179+10	.9089-5	.1633-2
83	.8835+8	.4828+8	.2321+10	.9219-5	.1371-2

z(km)	$[O_3]$	$[O_3]_n$	$[O_2(^1\Delta_g)]$	J_7	r_{59}
84	.7578+8	.5990+8	.2461+10	.9327-5	.1149-2
85	.6500+8	.6000+8	.2600+10	.9420-5	.9600-3
86	.3985+8	.5735+8	.2580+10	.9490-5	—
87	.2546+8	.5203+8	.2503+10	.9524-5	—
88	.1685+8	.4505+8	.2375+10	.9557-5	—
89	.1148+8	.3743+8	.2204+10	.9582-5	—
90	.8000+7	.3000+8	.2000+10	.9600-5	—
91	.5671+7	.2332+8	.1775+10	.9627-5	—
92	.4063+7	.1768+8	.1540+10	.9650-5	—
93	.2925+7	.1315+8	.1307+10	.9670-5	—
94	.2103+7	.9635+7	.1084+10	.9687-5	—
95	.1500+7	.7000+7	.8800+9	.9700-5	—
96	.1030+7	.5179+7	—	.9720-5	—
97	.6980+6	.3819+7	—	.9740-5	—
98	.4665+6	.2806+7	—	.9760-5	—
99	.3075+6	.2055+7	—	.9780-5	—
100	.2000+6	.1500+7	—	.9800-5	—

z(km)	$[O]_n$	$[NO^+]_n$	$[e^-]_n$	$[O_2^+]$	J_1	r_{31}
75	.7000+4	.2500+1	.6000+1	.7000+1	—	—
76	.4660+5	.2882+1	.1132+2	.9552+1	—	—
77	.3493+6	.3823+1	.1996+2	.1156+2	—	—
78	.2949+7	.5687+1	.3296+2	.1528+2	—	—
79	.2803+8	.7657+1	.5117+2	.3108+2	—	—
80	.3000+9	.1600+2	.7500+2	.5000+2	.1500-13	.1650-2
81	.8986+9	.3323+2	.1042+3	.9087+2	.2078-13	.2565-2
82	.2465+10	.6500+2	.1379+3	.1845+3	.2892-13	.4039-2
83	.6912+10	.1157+3	.1745+3	.3427+3	.3614-13	.6439-2
84	.1424+11	.1838+3	.2124+3	.6048+3	.4315-13	.1040-1
85	.3000+11	.2600+3	.2500+3	.1000+4	.5000-13	.1700-1
86	.5786+11	.3092+3	.2824+3	.1452+4	.5701-13	.2815-1
87	.1022+12	.3472+3	.3139+3	.2009+4	.6469-13	.4720-1
88	.1653+12	.3766+3	.3459+3	.2683+4	.7377-13	.7043-1
89	.2448+12	.4023+3	.3805+3	.3496+4	.8515-13	.1251+0
90	.3320+12	.4300+3	.4200+3	.4500+4	.1000-12	.2400+0
91	.4530+12	.4808+3	.4720+3	.6070+4	.1222-12	.5393+0
92	.5650+12	.5411+3	.5339+3	.8184+4	.1512-12	.1331+1
93	.6533+12	.6135+3	.6084+3	.1103+5	.1890-12	.3604+1
94	.7100+12	.7015+3	.6988+3	.1486+5	.2377-12	.1072+2
95	.7370+12	.8100+3	.8100+3	.2000+5	.3000-12	.3500+2
96	.7360+12	.9497+3	.9515+3	.2449+5	.3737-12	.3995+2
97	.7095+12	.1126+4	.1129+4	.2904+5	.4656-12	.4574+2
98	.6640+12	.1349+4	.1352+4	.3336+5	.5800-12	.5254+2
99	.6072+12	.1633+4	.1637+4	.3712+5	.7225-12	.6055+2
100	.5480+12	.2000+4	.2000+4	.4000+5	.9000-12	.7000+2

z(km)	$[e^-]$	$[NO^+]$	$[OH]_n$
55	.6000+1	—	—
56	.8846+1	—	—
57	.1335+2	—	—
58	.1802+2	—	—
59	.2229+2	—	—
60	.2800+2	—	.1500+6
61	.3274+2	—	.1500+6
62	.3707+2	—	.1500+6
63	.4096+2	—	.1500+6
64	.4453+2	—	.1500+6
65	.4800+2	—	.1500+6
66	.5336+2	—	.1500+6
67	.5929+2	—	.1500+6
68	.6583+2	—	.1500+6
69	.7304+2	—	.1500+6
70	.8100+2	.2500+3	.1500+6
71	.9296+2	.2692+3	.1401+6
72	.1079+3	.2890+3	.1301+6
73	.1309+3	.3091+3	.1199+6
74	.1540+3	.3295+3	.1099+6
75	.1800+3	.3500+3	.1000+6
76	.2048+3	.3706+3	.2273+6
77	.2307+3	.3910+3	.5240+6
78	.2473+3	.4111+3	.1226+7
79	.2756+3	.4309+3	.2908+7
80	.3100+3	.4500+3	.7000+7
81	.3606+3	.5570+3	.2153+7
82	.4253+3	.7152+3	.7806+6
83	.4957+3	.9456+3	.3337+6
84	.6055+3	.1277+4	.1682+6
85	.7600+3	.1750+4	.1000+6
86	.9966+3	.2341+4	.7248+5
87	.1451+4	.3152+4	.5253+5
88	.2045+4	.4272+4	.3807+5
89	.2877+4	.6150+4	.2759+5
90	.4000+4	.8000+4	.2000+5
91	.5212+4	.9388+4	.1450+5
92	.6397+4	.1068+5	.1051+5
93	.7926+4	.1186+5	.7615+4
94	.9758+4	.1295+5	.5519+4
95	.1200+5	.1400+5	.4000+4
96	.1514+5	.1554+5	.2801+4
97	.1918+5	.1721+5	.1939+4
98	.2440+5	.1900+5	.1326+4
99	.3118+5	.2093+5	.8973+3
100	.4000+5	.2300+5	.6000+3

z(km)	$[N_2O]$	$[O(^1D)]$
35	.7000+10	.5200+2
36	.4662+10	.6421+2
37	.3095+10	.7820+2
38	.2049+10	.9393+2
39	.1352+10	.1113+3
40	.8900+9	.1300+3
41	.5839+9	.1498+3
42	.3947+9	.1702+3
43	.2586+9	.1908+3
44	.1666+9	.2110+3
45	.1050+9	.2300+3
46	.6326+8	.2320+3
47	.3712+8	.2340+3
48	.2121+8	.2360+3
49	.1181+8	.2380+3
50	.6400+7	.2400+3

z(km)	J_{58}
35	.2920-4
36	.3394-4
37	.3901-4
38	.4439-4
39	.5001-4
40	.5580-4
41	.6170-4
42	.6765-4
43	.7355-4
44	.7936-4
45	.8500-4
46	.9057-4
47	.9585-4
48	.1007-3
49	.1052-3
50	.1090-3

z(km)	[M]	z(km)	[M]
35.5	.1624+18	81.5	.2890+15
36.5	.1401+18	82.5	.2417+15
37.5	.1210+18	83.5	.2017+15
38.5	.1046+18	84.5	.1682+15
39.5	.9055+17	85.5	.1404+15
40.5	.7850+17	86.5	.1174+15
41.5	.6815+17	87.5	.9826+14
42.5	.5926+17	88.5	.8222+14
43.5	.5158+17	89.5	.6881+14
44.5	.4494+17	90.5	.5783+14
45.5	.3920+17	91.5	.4827+14
46.5	.3421+17	92.5	.4003+14
47.5	.2989+17	93.5	.3335+14
48.5	.2605+17	94.5	.2782+14
49.5	.2285+17	95.5	.2328+14
50.5	.2013+17	96.5	.1955+14
51.5	.1792+17	97.5	.1644+14
52.5	.1595+17	98.5	.1384+14
53.5	.1422+17	99.5	.1166+14
54.5	.1267+17		
55.5	.1126+17		
56.5	.9979+16		
57.5	.8834+16		
58.5	.7807+16		
59.5	.6890+16		
60.5	.6072+16		
61.5	.5342+16		
62.5	.4693+16		
63.5	.4117+16		
64.5	.3607+16		
65.5	.3155+16		
66.5	.2756+16		
67.5	.2406+16		
68.5	.2096+16		
69.5	.1823+16		
70.5	.1583+16		
71.5	.1372+16		
72.5	.1188+16		
73.5	.1026+16		
74.5	.8849+15		
75.5	.7611+15		
76.5	.6547+15		
77.5	.5611+15		
78.5	.4792+15		
79.5	.4077+15		
80.5	.3451+15		

APPENDIX B

Odd Nitrogen Concentration Profiles

The equilibrium odd nitrogen concentration profiles resulting from all of the runs are included in this appendix. The values are those at the end of the daytime and nighttime integrations and are identified by the subscripts "D" and "N", respectively. The notation used to represent powers of ten is the following: value±x = value x $10^{\pm x}$. Units are cm^{-3}.

Model AL

	A=0.0		A=0.5		A=1.0	
z(km)	$[ON]_D$	$[ON]_N$	$[ON]_D$	$[ON]_N$	$[ON]_D$	$[ON]_N$
35	.1680+10	.1680+10	.1680+10	.1680+10	.1680+10	.1680+10
36	.1463+10	.1462+10	.1463+10	.1462+10	.1463+10	.1462+10
37	.1264+10	.1262+10	.1264+10	.1263+10	.1264+10	.1263+10
38	.1084+10	.1083+10	.1084+10	.1083+10	.1084+10	.1083+10
39	.9237+9	.9231+9	.9239+9	.9232+9	.9340+9	.9234+9
40	.7837+9	.7832+9	.7838+9	.7834+9	.7840+9	.7836+9
41	.6622+9	.6619+9	.6624+9	.6621+9	.6625+9	.6623+9
42	.5578+9	.5576+9	.5580+9	.5578+9	.5581+9	.5580+9
43	.4689+9	.4688+9	.4691+9	.4690+9	.4693+9	.4692+9
44	.3932+9	.3932+9	.3934+9	.3934+9	.3936+9	.3936+9
45	.3293+9	.3294+9	.3295+9	.3296+9	.3297+9	.3298+9
46	.2754+9	.2756+9	.2756+9	.2758+9	.2758+9	.2759+9
47	.2303+9	.2304+9	.2305+9	.2306+9	.2306+9	.2308+9
48	.1917+9	.1919+9	.1919+9	.1921+9	.1921+9	.1923+9
49	.1604+9	.1606+9	.1606+9	.1608+9	.1608+9	.1609+9
50	.1346+9	.1347+9	.1347+9	.1349+9	.1349+9	.1351+9
51	.1136+9	.1138+9	.1138+9	.1140+9	.1140+9	.1141+9
52	.9606+8	.9624+8	.9623+8	.9641+8	.9641+8	.9658+8
53	.8127+8	.8145+8	.8144+8	.8162+8	.8161+8	.8179+8
54	.6875+8	.6893+8	.6892+8	.6909+8	.6909+8	.6927+8
55	.5811+8	.5829+8	.5828+8	.5846+8	.5845+8	.5863+8
56	.4886+8	.4904+8	.4903+8	.4920+8	.4919+8	.4937+8
57	.4103+8	.4120+8	.4119+8	.4137+8	.4136+8	.4153+8
58	.3444+8	.3461+8	.3460+8	.3477+8	.3476+8	.3493+8
59	.2888+8	.2905+8	.2905+8	.2921+8	.2920+8	.2937+8
60	.2422+8	.2439+8	.2439+8	.2455+8	.2455+8	.2471+8
61	.2033+8	.2049+8	.2049+8	.2065+8	.2065+8	.2081+8
62	.1709+8	.1724+8	.1725+8	.1741+8	.1741+8	.1757+8
63	.1440+8	.1455+8	.1456+8	.1472+8	.1472+8	.1488+8
64	.1218+8	.1232+8	.1234+8	.1249+8	.1250+8	.1266+8
65	.1035+8	.1049+8	.1052+8	.1067+8	.1068+8	.1084+8
66	.8857+7	.8997+7	.9031+7	.9176+7	.9195+7	.9346+7
67	.7638+7	.7777+7	.7816+7	.7960+7	.7983+7	.8134+7
68	.6650+7	.6789+7	.6832+7	.6978+7	.7004+7	.7157+7

Model AL

	A=0.0		A=0.5		A=1.0	
z(km)	$[ON]_D$	$[ON]_N$	$[ON]_D$	$[ON]_N$	$[ON]_D$	$[ON]_N$
69	.5849+7	.5989+7	.6037+7	.6185+7	.6213+7	.6370+7
70	.5205+7	.5347+7	.5398+7	.5551+7	.5580+7	.5743+7
71	.4688+7	.4836+7	.4888+7	.5048+7	.5077+7	.5250+7
72	.4281+7	.4437+7	.4490+7	.4660+7	.4687+7	.4872+7
73	.3961+7	.4126+7	.4178+7	.4361+7	.4384+7	.4585+7
74	.3713+7	.3889+7	.3941+7	.4138+7	.4158+7	.4376+7
75	.3525+7	.3714+7	.3764+7	.3978+7	.3993+7	.4231+7
76	.3383+7	.3586+7	.3635+7	.3867+7	.3877+7	.4137+7
77	.3291+7	.3506+7	.3559+7	.3807+7	.3817+7	.4098+7
78	.3228+7	.3445+7	.3511+7	.3767+7	.3784+7	.4080+7
79	.3192+7	.3399+7	.3491+7	.3745+7	.3781+7	.4083+7
80	.3179+7	.3364+7	.3494+7	.3737+7	.3800+7	.4104+7
81	.3140+7	.3341+7	.3473+7	.3747+7	.3798+7	.4149+7
82	.3117+7	.3380+7	.3475+7	.3833+7	.3826+7	.4284+7
83	.3115+7	.3494+7	.3506+7	.4012+7	.3894+7	.4530+7
84	.3150+7	.3706+7	.3588+7	.4311+7	.4026+7	.4918+7
85	.3245+7	.4052+7	.3749+7	.4770+7	.4255+7	.5493+7
86	.3439+7	.4589+7	.4036+7	.5454+7	.4638+7	.6329+7
87	.3783+7	.5357+7	.4508+7	.6406+7	.5244+7	.7468+7
88	.4334+7	.6430+7	.5236+7	.7699+7	.6151+7	.8984+7
89	.5151+7	.7907+7	.6281+7	.9430+7	.7430+7	.1097+8
90	.6341+7	.9975+7	.7760+7	.1179+8	.9200+7	.1362+8
91	.7802+7	.1259+8	.9533+7	.1467+8	.1129+8	.1677+8
92	.9580+7	.1592+8	.1164+8	.1823+8	.1373+8	.2056+8
93	.1181+8	.2033+8	.1425+8	.2280+8	.1671+8	.2529+8
94	.1457+8	.2593+8	.1741+8	.2844+8	.2027+8	.3096+8
95	.1808+8	.3278+8	.2132+8	.3517+8	.2459+8	.3759+8
96	.2280+8	.4086+8	.2640+8	.4298+8	.3004+8	.4512+8
97	.2944+8	.4969+8	.3321+8	.5137+8	.3700+8	.5307+8
98	.3910+8	.5864+8	.4260+8	.5978+8	.4611+8	.6092+8
99	.5331+8	.6697+8	.5572+8	.6752+8	.5814+8	.6807+8
100	.7400+8	.7400+8	.7400+8	.7400+8	.7400+8	.7400+8

Model AH

	A=0.0		A=0.5		A=1.0	
z(km)	$[ON]_D$	$[ON]_N$	$[ON]_D$	$[ON]_N$	$[ON]_D$	$[ON]_N$
35	.1680+10	.1680+10	.1680+10	.1680+10	.1680+10	.1680+10
36	.1464+10	.1463+10	.1464+10	.1463+10	.1464+10	.1463+10
37	.1265+10	.1264+10	.1265+10	.1264+10	.1265+10	.1264+10
38	.1086+10	.1085+10	.1086+10	.1085+10	.1086+10	.1085+10
39	.9264+9	.9258+9	.9266+9	.9259+9	.9267+9	.9261+9
40	.7868+9	.7863+9	.7869+9	.7864+9	.7870+9	.7866+9
41	.6656+9	.6653+9	.6658+9	.6655+9	.6659+9	.6656+9
42	.5614+9	.5612+9	.5615+9	.5614+9	.5617+9	.5615+9
43	.4727+9	.4726+9	.4728+9	.4727+9	.4730+9	.4729+9
44	.3970+9	.3971+9	.3972+9	.3972+9	.3973+9	.3974+9
45	.3331+9	.3332+9	.3333+9	.3334+9	.3334+9	.3335+9
46	.2792+9	.2794+9	.2794+9	.2795+9	.2795+9	.2797+9
47	.2340+9	.2342+9	.2341+9	.2343+9	.2343+9	.2344+9
48	.1954+9	.1955+9	.1955+9	.1957+9	.1956+9	.1958+9
49	.1640+9	.1641+9	.1641+9	.1643+9	.1642+9	.1644+9
50	.1380+9	.1382+9	.1381+9	.1383+9	.1383+9	.1384+9
51	.1170+9	.1172+9	.1171+9	.1173+9	.1173+9	.1174+9
52	.9943+8	.9961+8	.9956+8	.9974+8	.9968+8	.9986+8
53	.8460+8	.8479+8	.8472+8	.8491+8	.8484+8	.8503+8
54	.7205+8	.7224+8	.7217+8	.7236+8	.7229+8	.7248+8
55	.6139+8	.6158+8	.6151+8	.6170+8	.6162+8	.6182+8
56	.5210+8	.5230+8	.5222+8	.5242+8	.5233+8	.5253+8
57	.4424+8	.4444+8	.4436+8	.4456+8	.4446+8	.4466+8
58	.3763+8	.3783+8	.3774+8	.3794+8	.3784+8	.3805+8
59	.3206+8	.3226+8	.3217+8	.3237+8	.3227+8	.3248+8
60	.2740+8	.2760+8	.2751+8	.2771+8	.2761+8	.2782+8
61	.2351+8	.2372+8	.2362+8	.2383+8	.2372+8	.2393+8
62	.2028+8	.2049+8	.2039+8	.2061+8	.2049+8	.2071+8
63	.1762+8	.1784+8	.1773+8	.1796+8	.1784+8	.1806+8
64	.1545+8	.1568+8	.1556+8	.1579+8	.1566+8	.1590+8
65	.1368+8	.1393+8	.1379+8	.1404+8	.1390+8	.1416+8
66	.1226+8	.1253+8	.1238+8	.1265+8	.1249+8	.1277+8
67	.1114+8	.1143+8	.1126+8	.1156+8	.1138+8	.1168+8
68	.1028+8	.1059+8	.1040+8	.1073+8	.1052+8	.1086+8
69	.9617+7	.9979+7	.9750+7	.1012+8	.9879+7	.1026+8
70	.9143+7	.9560+7	.9282+7	.9712+7	.9419+7	.9861+7
71	.8826+7	.9318+7	.8975+7	.9483+7	.9122+7	.9645+7
72	.8663+7	.9250+7	.8823+7	.9430+7	.8980+7	.9608+7
73	.8627+7	.9332+7	.8801+7	.9533+7	.8972+7	.9730+7
74	.8720+7	.9567+7	.8910+7	.9791+7	.9098+7	.1001+8
75	.8933+7	.9952+7	.9144+7	.1021+8	.9353+7	.1046+8
76	.9257+7	.1048+8	.9492+7	.1077+8	.9724+7	.1106+8
77	.9722+7	.1120+8	.9987+7	.1154+8	.1025+8	.1187+8
78	.1028+8	.1206+8	.1057+8	.1245+8	.1087+8	.1283+8
79	.1093+8	.1309+8	.1127+8	.1353+8	.1160+8	.1398+8
80	.1167+8	.1430+8	.1205+8	.1482+8	.1243+8	.1533+8
81	.1243+8	.1565+8	.1286+8	.1625+8	.1329+8	.1684+8

Model AH

	A=0.0		A=0.5		A=1.0	
z(km)	$[ON]_D$	$[ON]_N$	$[ON]_D$	$[ON]_N$	$[ON]_D$	$[ON]_N$
82	.1330+8	.1725+8	.1378+8	.1795+8	.1426+8	.1865+8
83	.1431+8	.1915+8	.1486+8	.1996+8	.1540+8	.2078+8
84	.1552+8	.2139+8	.1613+8	.2233+8	.1673+8	.2328+8
85	.1693+8	.2402+8	.1762+8	.2511+8	.1831+8	.2620+8
86	.1862+8	.2719+8	.1941+8	.2844+8	.2021+8	.2968+8
87	.2054+8	.3085+8	.2146+8	.3224+8	.2237+8	.3362+8
88	.2265+8	.3502+8	.2372+8	.3652+8	.2479+8	.3802+8
89	.2494+8	.3966+8	.2619+8	.4123+8	.2745+8	.4281+8
90	.2754+8	.4492+8	.2902+8	.4653+8	.3049+8	.4814+8
91	.3007+8	.4998+8	.3176+8	.5154+8	.3345+8	.5310+8
92	.3262+8	.5469+8	.3451+8	.5614+8	.3641+8	.5759+8
93	.3560+8	.5938+8	.3768+8	.6067+8	.3976+8	.6197+8
94	.3899+8	.6364+8	.4121+8	.6474+8	.4343+8	.6585+8
95	.4289+8	.6730+8	.4518+8	.6819+8	.4748+8	.6909+8
96	.4752+8	.7041+8	.4979+8	.7109+8	.5206+8	.7178+8
97	.5285+8	.7265+8	.5495+8	.7313+8	.5704+8	.7361+8
98	.5897+8	.7397+8	.6068+8	.7427+8	.6239+8	.7456+8
99	.6598+8	.7439+8	.6701+8	.7453+8	.6805+8	.7466+8
100	.7400+8	.7400+8	.7400+8	.7400+8	.7400+8	.7400+8

	Model BL		Model BH	
	A=0.5		A=0.5	
z(km)	$[ON]_D$	$[ON]_N$	$[ON]_D$	$[ON]_N$
35	.1680+10	.1680+10	.1680+10	.1680+10
36	.1563+10	.1562+10	.1574+10	.1573+10
37	.1404+10	.1403+10	.1422+10	.1421+10
38	.1228+10	.1227+10	.1250+10	.1250+10
39	.1052+10	.1051+10	.1077+10	.1076+10
40	.8873+9	.8869+9	.9124+9	.9119+9
41	.7389+9	.7386+9	.7628+9	.7624+9
42	.6093+9	.6092+9	.6311+9	.6310+9
43	.4988+9	.4988+9	.5182+9	.5182+9
44	.4057+9	.4058+9	.4228+9	.4228+9
45	.3287+9	.3288+9	.3434+9	.3435+9
46	.2655+9	.2656+9	.2781+9	.2783+9
47	.2142+9	.2143+9	.2250+9	.2252+9
48	.1721+9	.1722+9	.1813+9	.1814+9
49	.1388+9	.1390+9	.1468+9	.1469+9
50	.1123+9	.1124+9	.1191+9	.1192+9
51	.9155+8	.9166+8	.9751+8	.9763+8
52	.7491+8	.7502+8	.8020+8	.8031+8
53	.6149+8	.6159+8	.6622+8	.6633+8
54	.5062+8	.5071+8	.5490+8	.5501+8
55	.4177+8	.4186+8	.4572+8	.4583+8
56	.3441+8	.3450+8	.3808+8	.3818+8
57	.2841+8	.2850+8	.3187+8	.3198+8

	Model BL		Model BH	
	A=0.5		A=0.5	
z(km)	$[ON]_D$	$[ON]_N$	$[ON]_D$	$[ON]_N$
58	.2355+8	.2363+8	.2685+8	.2696+8
59	.1960+8	.1968+8	.2279+8	.2289+8
60	.1639+8	.1647+8	.1950+8	.1961+8
61	.1379+8	.1386+8	.1686+8	.1697+8
62	.1169+8	.1176+8	.1474+8	.1485+8
63	.9987+7	.1006+8	.1305+8	.1317+8
64	.8618+7	.8692+7	.1171+8	.1185+8
65	.7517+7	.7594+7	.1067+8	.1082+8
66	.6635+7	.6715+7	.9865+7	.1004+8
67	.5929+7	.6014+7	.9265+7	.9466+7
68	.5368+7	.5459+7	.8836+7	.9076+7
69	.4920+7	.5020+7	.8550+7	.8839+7
70	.4566+7	.4676+7	.8390+7	.8745+7
71	.4286+7	.4411+7	.8342+7	.8785+7
72	.4073+7	.4214+7	.8409+7	.8964+7
73	.3908+7	.4069+7	.8573+7	.9272+7
74	.3786+7	.3968+7	.8842+7	.9712+7
75	.3697+7	.3903+7	.9212+7	.1029+8
76	.3631+7	.3862+7	.9669+7	.1099+8
77	.3598+7	.3851+7	.1025+8	.1186+8
78	.3574+7	.3840+7	.1088+8	.1284+8
79	.3561+7	.3826+7	.1158+8	.1394+8
80	.3554+7	.3808+7	.1231+8	.1516+8
81	.3515+7	.3799+7	.1303+8	.1649+8
82	.3504+7	.3870+7	.1390+8	.1811+8
83	.3526+7	.4038+7	.1493+8	.2008+8
84	.3602+7	.4329+7	.1618+8	.2241+8
85	.3758+7	.4782+7	.1766+8	.2516+8
86	.4041+7	.5463+7	.1944+8	.2847+8
87	.4512+7	.6412+7	.2147+8	.3226+8
88	.5238+7	.7703+7	.2373+8	.3654+8
89	.6283+7	.9432+7	.2620+8	.4124+8
90	.7761+7	.1179+8	.2902+8	.4654+8
91	.9533+7	.1467+8	.3176+8	.5155+8
92	.1164+8	.1823+8	.3452+8	.5614+8
93	.1425+8	.2280+8	.3768+8	.6068+8
94	.1741+8	.2844+8	.4121+8	.6475+8
95	.2132+8	.3517+8	.4518+8	.6819+8
96	.2640+8	.4298+8	.4979+8	.7110+8
97	.3321+8	.5137+8	.5495+8	.7313+8
98	.4260+8	.5978+8	.6068+8	.7427+8
99	.5572+8	.6752+8	.6701+8	.7453+8
100	.7400+8	.7400+8	.7400+8	.7400+8

REFERENCES

Anderson, J.G. (1971) Rocket measurement of OH in the mesosphere. J. Geophys. Res., 76, 7820.

Banks, P.M., and G. Kockarts (1973) Aeronomy, Part A. Academic Press, New York, p. 322.

Barth, C.A. (1966) Nitric oxide in the upper atmosphere. Ann. Geophys., 22, 198.

Baulch, D.L., D.D. Drysdale, and D.G. Horne (1973) The reaction of N with O_2, in Chemical kinetics data survey, 5. Sixty-six contributed rate and photochemical data evaluations on ninety-four reactions. NBSIR 73-206. Edited by D. Garvin, Natl. Bur. of Stand., Washington, D.C.

Baulch, D.L., D.D. Drysdale, and D.G. Horne (1973) The reaction of nitrogen atom with ozone. Ibid.

Baulch, D.L., D.D. Drysdale, and D.G. Horne (1973) The combination of NO and O. Ibid.

Baulch, D.L., D.D. Drysdale, and D.G. Horne (1973) The reaction of nitrogen atom with hydroxyl. Ibid.

Becker, K.H., W. Groth, and D. Thran (1973) Mechanism of the air afterglow $NO + O \rightarrow NO_2 + h\nu$, in Symp. Combust. 14th. Combustion Institute, Pittsburgh, p. 353.

Brasseur, G., and M. Nicolet (1973) Chemospheric processes of nitric oxide in the mesosphere and stratosphere. Planet. Space Sci., 21, 939.

Cieslik, S., and M. Nicolet (1973) The aeronomic dissociation of nitric oxide. Planet. Space Sci., 21, 925.

Clark, I.D., and R.P. Wayne (1970) Kinetics of the reaction between atomic nitrogen and molecular oxygen in the ground ($^3\Sigma g^-$) and first excited ($^1\Delta_g$) states. Proc. Roy. Soc. London, A316, 539.

Colegrove, F.D., F.S. Johnson, and W.B. Hanson (1966) Atmospheric composition in the lower thermosphere. J. Geophys. Res., 71, 2227.

Cospar International Reference Atmosphere, 1965. Committee on Space Research, The International Council of Scientific Unions. North-Holland, Amsterdam, pp. 9, 12.

Davenport, J.E., T.G. Slanger, and G. Black (1976) The quenching of $N(^2D)$ by $O(^3P)$. J. Geophys. Res., 81, 12.

Davis, D., J. Herron, and R. Huie (1973) Absolute rate constants for the reaction $O + NO_2 \rightarrow NO + O_2$ over the temperature range 230-339°K. J. Chem. Phys., 58, 530.

Ehhalt, D.H., L.E. Heidt, R.H. Lueb, and N. Roper (1974) Vertical profiles of CH_4, H_2, CO, N_2O and CO_2 in the stratosphere. Proceedings of the Third Conference on the Climatic Impact Assessment Program, DOT-TSC-OST-74-15. Edited by A.J. Broderick and T.M. Hard, Natl. Tech. Inform. Serv., Springfield, VA, p. 153.

Ehhalt, D.H., L.E. Heidt, R.H. Lueb, and E.A. Martell (1975) Concentrations of CH_4, CO, CO_2, H_2, H_2O and N_2O in the upper stratosphere. J. Atmos. Sci., 32, 163.

Garvin, D., and R.F. Hampson, editors (1974) Chemical kinetics data survey, 7.Tables of rate and photochemical data for modelling of the stratosphere. NBSIR 74-430. Natl. Bur. of Stand., Washington, D.C.

Goldan, P.D., A.L. Schmeltekopf, F.C. Fehsenfeld, H.I. Schiff, and E.E. Ferguson (1966) Thermal-energy ion-neutral reaction rates, 2. Some reactions of ionospheric interest. J. Chem. Phys., 44, 4095.

Henderson, W.R. (1971) D-region atomic oxygen measurement. J. Geophys. Res., 76, 3166.

Herron, J.T., and R.E. Huie (1972) The reaction between NO and O_3, in Chemical kinetics data survey, 2. Photochemical and rate data for fifteen gas phase reactions of interest for stratospheric chemistry. Rep. 10828. Edited by R.F. Hampson, Natl. Bur. of Stand., Washington, D.C.

Huang, C., M.A. Biondi, and R. Johnsen (1975) Variation of electron-NO^+ ion-recombination coefficient with electron temperatures. Phys. Rev. A, 11, 901.

Hunten, D.M. (1975) Vertical transport in atmospheres. In Atmospheres of Earth and the Planets. Edited by B.M. McCormac; D. Reidel, Dordrecht-Holland, p. 59.

Hunten, D.M., and D.F. Strobel (1974) Production and escape of terrestrial hydrogen. J. Atmos. Sci., 31, 305.

Husain, D., L.J. Kirsch, and J.R. Wiesenfeld (1972) Collisional quenching of electronically excited nitrogen atoms N (2^2D_J, 2^2P_J) by time-resolved atomic absorption spectroscopy. Discuss. Faraday Soc., 53, 201.

Jacchia, L.G. (1971) Revised static models of the thermosphere and exosphere with empirical temperature profiles. Special Report 332, Smithsonian Astrophysical Observatory, Cambridge, MA.

Johnson, C.Y. (1966) Ionospheric composition and density from 90 to 1200 kilometers at solar minimum. J. Geophys. Res., 71, 330.

Keneshea, T.J., R.S. Narcisi, and W. Swider (1970) Diurnal model of the E region. J. Geophys. Res., 75, 845.

Llewellyn, E.J., W.F.J. Evans, and H.C. Wood (1973) O_2 ($^1\Delta$) in the atmosphere. In Physics and Chemistry of Upper Atmospheres. Edited by B.M. McCormac; D. Reidel, Dordrecht-Holland, p. 193.

Lorenz, E.N. (1971) An N-cycle time-differencing scheme for stepwise numerical integration. Mon. Weather Rev., 99, 644.

McConnell, J.C., and M.B. McElroy (1973) Odd nitrogen in the atmosphere. J. Atmos. Sci., 30, 1465.

McEwan, M.J., and L.F. Phillips (1975) Chemistry of the Atmosphere. John Wiley and Sons, New York.

McFarland, M., D.L. Albritton, F.C. Fehsenfeld, E.E. Ferguson, and A.L. Schmeltekopf (1973) A flow-drift technique for ion mobility and ion-molecule reaction rate constant measurements, 2. The positive ion reactions of N^+, O^+ and N_2^+ with O_2 and O^+ with N_2 from thermal to $\sim$ 2 eV. J. Chem. Phys., 59, 6620.

McFarland, M., D.L. Albritton, F.C. Fehsenfeld, E.E. Ferguson, and A.L. Schmeltekopf (1974) Energy dependence and branching ratio of the $N_2^+ + O$ reaction. J. Geophys. Res., 79, 2925.

Mechtly, E.A., and L.G. Smith (1968) Seasonal variation of the lower ionosphere at Wallops Island during the IQSY. J. Atmos. Terr. Phys., 30, 1555.

Meira, L.G. (1971) Rocket measurements of upper atmospheric nitric oxide and their consequences to the lower ionosphere. NASA CR-1690, prepared for NASA, under Contract No. NGL-06-003-064, by University of Colorado. Natl. Tech. Inform. Serv., Springfield, VA, p. 53.

Narcisi, R.S. (1973) Mass spectrometer measurements in the ionosphere. In Physics and Chemistry of Upper Atmospheres. Edited by B.M. McCormac; D. Reidel, Dordrecht-Holland, p. 171.

Narcisi, R.S., and A.D. Bailey (1965) Mass spectrometric measurements of positive ions at altitudes from 64 to 112 kilometers. J. Geophys. Res., 70, 3687.

Nicolet, M. (1971) Aeronomic reactions of hydrogen and ozone. In Mesospheric Models and Related Experiments. Edited by G. Fiocco; D. Reidel, Dordrecht-Holland, p. 1.

Nicolet, M. (1975) On the production of nitric oxide by cosmic rays in the mesosphere and stratosphere. Planet. Space Sci., 23, 637.

Norton, R.B., and C.A. Barth (1970) Theory of nitric oxide in the earth's atmosphere. J. Geophys. Res., 75, 3903.

Ogawa, T., and T. Shimazaki (1975) Diurnal variations of odd nitrogen and ionic densities in the mesosphere and lower thermosphere: simultaneous solution of photochemical-diffusive equations. J. Geophys. Res., 80, 3945.

Oran, E.S., P.S. Julienne, and D.F. Strobel (1975) The aeronomy of odd nitrogen in the thermosphere. J. Geophys. Res., 80, 3068.

Phillips, L.F., and H.I. Schiff (1962) Mass spectrometric studies of atom reactions, 1. Reactions in the atomic nitrogen-ozone system. J. Chem. Phys., 36, 1509.

Phillips, L.F., and H.I. Schiff (1965) Mass-spectrometric studies of atomic reactions, 5. The reaction of nitrogen atoms with NO_2. J. Chem. Phys., 42, 3171.

Prinn, R.G., F.N. Alyea, and D.M. Cunnold (1975) Stratospheric distributions of odd nitrogen and odd hydrogen in a two-dimensional model. J. Geophys. Res., 80, 4997.

Reid, G.C. (1971) The roles of water vapor and nitric oxide in determining electron densities in the D-region. In Mesospheric Models and Related Experiments. Edited by G. Fiocco; D. Reidel, Dordrecht-Holland, p. 198.

Ridley, B.A. (1977) Stratospheric measurements of nitrogen oxides. NASA position paper, unpublished, York University, Toronto.

Slanger, T.G., B.J. Wood, and G. Black (1971) Temperature coefficients for $N(^2D)$ quenching by O_2 and N_2O. J. Geophys. Res., 76, 8430.

Strobel, D.F. (1971a) Diurnal variation of nitric oxide in the upper atmosphere. J. Geophys. Res., 76, 2441.

Strobel, D.F. (1971b) Odd nitrogen in the mesosphere. J. Geophys. Res., 76, 8384.

Strobel, D.F. (1972a) Minor neutral constituents in the mesosphere and lower thermosphere. Radio Sci., 7, 1.

Strobel, D.F. (1972b) Nitric oxide in the D region. J. Geophys. Res., 77, 1337.

Strobel, D.F., D.M. Hunten, and M.B. McElroy (1970) Production and diffusion of nitric oxide. J. Geophys. Res., 75, 4307.

Strobel, D.F., E.S. Oran, and P.D. Feldman (1975) The aeronomy of odd nitrogen in the thermosphere, 2. Twilight emissions. NRL Memorandum Report 3090. Naval Research Laboratory, Washington, D.C.

Thomas, L. (1973) The oxygen-hydrogen atmosphere. In Physics and Chemistry of Upper Atmospheres. Edited by B.M. McCormac; D. Reidel, Dordrecht-Holland, p. 133.

von Zahn, U., H. Trinks, and D. Offermann (1977) Neutral composition measurements between 90 and 220 km by rocket borne mass spectrometer (abstract). Eos Trans. AGU, 58, 455.

Wu, M-F (1974) Trace constituents in the stratosphere. Tech. report prepared for Dept. of Transportation, CIAP, under Contract No. DOT-OS-20217, by Environmental Research and Technology, Inc., Lexington, MA.

ACKNOWLEDGEMENTS

I am very grateful to my wife, Ellyn, for the many sacrifices she had to make in order for me to do this research and write this thesis.

I would also like to thank Professor Edward Lorenz, Doctor Derek Cunnold, and Professor Ronald Prinn for several useful discussions.

My appreciation is further extended to Sam Ricci for drafting the figures and Cheri Pierce for typing most of the manuscript.

This work was supported by NASA Grant NSG-2010.